

Studies on Multinuclear Magnesium *tert*-Butyl Heteroscorpionates: Synthesis, Coordination Ability and Heteroselective ROP of *rac*-Lactide

Andrés Garcés,[†] Luis F. Sánchez-Barba,^{†} Juan Fernández-Baeza,[‡] Antonio Otero,^{*‡} Manuel
Honrado,[‡] Agustín Lara-Sánchez,[‡] and Ana M. Rodríguez[‡]*

[†]Departamento de Biología y Geología, Física y Química Inorgánica, Universidad Rey Juan Carlos, Móstoles-28933-Madrid, Spain.

[‡] Universidad de Castilla-La Mancha, Departamento de Química Inorgánica, Orgánica y Bioquímica-Centro de Innovación en Química Avanzada (ORFEO-CINQA), Campus Universitario, 13071-Ciudad Real, Spain.

E-mail: luisfernando.sanchezbarba@urjc.es, antonio.otero@uclm.es;

RECEIVED DATE (to be automatically inserted after your manuscript is accepted if required according to the journal that you are submitting your paper to)

“This document is the unedited Author’s version of a Submitted Work that was subsequently accepted for publication in *Organometallics*, copyright © American Chemical Society after peer review. To access the final edited and published work see

<http://pubs.acs.org/articlesonrequest/AOR-qvUePYIkXq73mn9jGdNp.>”

ABSTRACT

The reaction of the low sterically hindered heteroscorpionate lithium acetamidates [Li(κ^3 -NNN)(thf)] {NNN = pbpamd (**1**) [pbpamd = *N,N'*-diisopropylbis(3,5-dimethylpyrazol-1-yl)acetamidate], tbpamd (**2**) [tbpamd = *N*-ethyl-*N'*-*tert*-butylbis(3,5-dimethylpyrazol-1-yl)acetamidate], ttbpamd (**3**) [ttbpamd = *N,N'*-di-*tert*-butylbis(3,5-dimethylpyrazol-1-yl)acetamidate], phbpamd (**4**) [phbpamd = *N,N'*-di-*p*-tolylbis(3,5-dimethylpyrazol-1-yl)acetamidate]} and the highly sterically demanding [Li(κ^3 -phbp'amd)(thf)] (**5**) [phbp'amd = *N,N'*-di-*p*-tolylbis(3,5-di-*tert*-butylpyrazol-1-yl)acetamidate] with the commercially available Grignard reagent ^tBuMgCl in an equimolecular ratio yielded the magnesium *tert*-butyl compounds [Mg(^tBu)(κ^3 -NNN)] [NNN = pbpamd (**6**), tbpamd (**7**), ttbpamd (**8**), and phbp'amd (**9**)]. In addition, subsequent reaction of the monoalkyls **6–8** with two additional equivalents of ^tBuMgCl in a mixture of tetrahydrofuran/dioxane gave rise to two different classes of chiral compounds, namely the tetranuclear complexes [{(^tBu)Mg(κ^3 -*N,N,N*; κ^2 -*C,N*)Mg(^tBu)}₂{ μ -*O,O*-(C₄H₈)}] (κ^3 -*N,N,N*; κ^2 -*C,N* = pbpamd⁻ **10**, tbpamd⁻ **11a**) and [(^tBu)Mg(κ^2 -*N,N*; κ^2 -*N,N*)Mg(^tBu){ μ -*O,O*-(C₄H₈)}]₂ (κ^2 -*N,N*; κ^2 -*N,N* = tbpamd⁻ **11b**). This reaction for **8** was unsuccessful but an analog such as the dinuclear complex [(thf)(^tBu)Mg(κ^2 -*N,N*; κ^2 -*N,N*)Mg(^tBu)(thf)] (κ^2 -*N,N*; κ^2 -*N,N* = phbpamd⁻ **12**) could be obtained from its lithium salt. In all cases (**10–12**) an apical methane C–H activation on the heteroscorpionate takes place. This process was not observed for complex **9** but, interestingly, the coordination of one additional equivalent of Mg^tBu₂ afforded the dinuclear complex [Mg(^tBu)(κ^3 -phbp'amd){Mg(^tBu)₂}] (**13**). Similarly, coordination of Mg^tBu₂ to **10** produces the chiral trinuclear [{(^tBu)Mg(pbpamd⁻)Mg(^tBu)}₂{ μ -*O,O*-(C₄H₈)}₂{Mg(^tBu)₂(thf)}] (**14**). The X-ray crystal structures of complexes **4**, **6**, **8**, **9**, **11b**, **12**, **13** and **14** confirm the nuclearity of each family and the existence of apical σ -C(*sp*³)–Mg (**14**) and extended π -C₂N₂(*sp*²)–Mg₂ (**11b** and **12**) covalent bonds have unambiguously been confirmed. Interestingly, the mononuclear compounds **8** and **9**, the tetranuclear compound **10**, and the dinuclear compounds **12** and **13** can act as highly efficient single-component living initiators for the ROP of *rac*-lactide. The most

sterically hindered initiators exhibit enhanced levels of heteroselectivity on the PLAs, with **9** reaching P_s values up to 0.85.

Introduction

Biosourced polylactide (PLA)¹ (including its copolymers) is a leading commercial biomaterial, the production of which has increased annually (nearly doubling from 0.7 million tonnes in 2014 to well over 1.2 million tonnes in 2019).² The increasing interest in this area is evidenced by the number of reviews³ and books⁴ that have recently been published in this field. Considering the biomedical/pharmaceutical applications, *e.g.*, in regenerative medicine,⁵ controlled release of drugs⁶ and wound healing,⁷ which are due to the biocompatible nature and the non-toxicity to living tissue of bioassimilable polylactides (PLAs), the use of biologically benign metal-based catalysts such as zinc^{8a,b} and magnesium^{8c,d} is widespread. In addition, ecological applications as bulk commodity materials⁹ have recently appeared for this emerging type of biodegradable material.

In recent years our research group has explored the synthesis of well-defined alkyl magnesium¹⁰ and alkyl¹¹-amide¹² zinc complexes supported by amidinate-based scorpionate ligands of the type $[M(R)(\kappa^3\text{-NNN})]$ ($M = \text{Mg, Zn}$; $R = \text{alkyl, amide}$) as efficient single-component living initiators for the ROP of lactides.¹³ During this time we demonstrated that the lack of steric influence of the substituents on the heteroscorpionate ligands facilitates the metal complexes undergoing the symmetrical equilibrium (Schlenk equilibrium:¹⁴ $2 \text{RMgX} \rightleftharpoons \text{MgR}_2 + \text{MgX}_2$) to form sandwich species that dramatically disfavor catalytic performance.¹⁵ We have also shown that the architecture of complexes with more sterically hindered environments¹⁶ or higher order nuclearity arrangements¹⁰ provides a steric barrier to suppress this undesired side reaction. In particular, we recently studied¹⁰ this latter approach through C–H activation (deprotonation) of the bridging methine in the previously reported magnesium monoalkyls $[Mg(R)(\kappa^3\text{-NNN})]$,¹⁵ which gave PLA materials with a moderate increase in the level of heteroselectivity ($P_r = 0.79$).¹⁰ In addition, several reports have recently been published concerning this methine C–H

activation process and these include group 3 (Sc, Y),¹⁷ lanthanide (Lu,¹⁷ Nd)¹⁸ and group 13 (Al)¹⁹-based alternative heteroscorpionate complexes. In these studies, very interesting results were obtained in the production of enriched heterotactic¹⁷ ($P_s = 0.81$, Y; 0.87, Lu) and isotactic¹⁸ ($P_i = 0.61$, conv 10%) poly(*rac*-LAs), as well as for the synthesis of cyclic carbonates.^{19,20}

On the other hand, it is well established²¹ that the composition of a Grignard reagent (RMgX) depends on the nature of the organic group, the halide and the solvent, as well as the temperature and the concentration, although the effect of solvent seems to play a dominant role in deciding the position of the Schlenk equilibrium¹⁴ (*i.e.*, monomeric arrangements in tetrahydrofuran *vs.* association processes in diethyl ether). In contrast, the alkyl group has very little effect on the position of the equilibrium, although *tert*-butyl magnesium chloride shows quite different behavior in that and it has an equal ratio of the participants in the equilibrium in tetrahydrofuran (equilibrium constant, K of 1.12 at 33°C).²² The study of the influence of the two factors described above on the position of the symmetrical equilibrium¹⁴ for the alkyl magnesium complexes requires the use of both the new amidinate-based heteroscorpionate ligands prepared and ^tBuMgCl, the Grignard reagent that shows different behavior, in the search for more selective and effective magnesium-based initiators for the ROP of lactide. This encouraged us to focus our initial studies on the architecture of species with higher order nuclearity through a C–H activation process.¹⁰

We describe here progress in the study of the exceptional reactivity of the Grignard reagent ^tBuMgCl with new low and high sterically hindered amidinate-based heteroscorpionates. In this case, cleavage of the apical methine C–H bond led to the formation of both apical carbanions with direct $\sigma\text{-C}(sp^3)\text{-Mg}$ and extended $\pi\text{-C}_2\text{N}_2(sp^2)\text{-Mg}_2$ covalent bonds in the isolated species. The different reactivity levels and the unique structural arrangements elucidated in the complexes are discussed along with their ability to act as effective single-component living initiators for the production of heteroenriched PLAs from *rac*-LA.

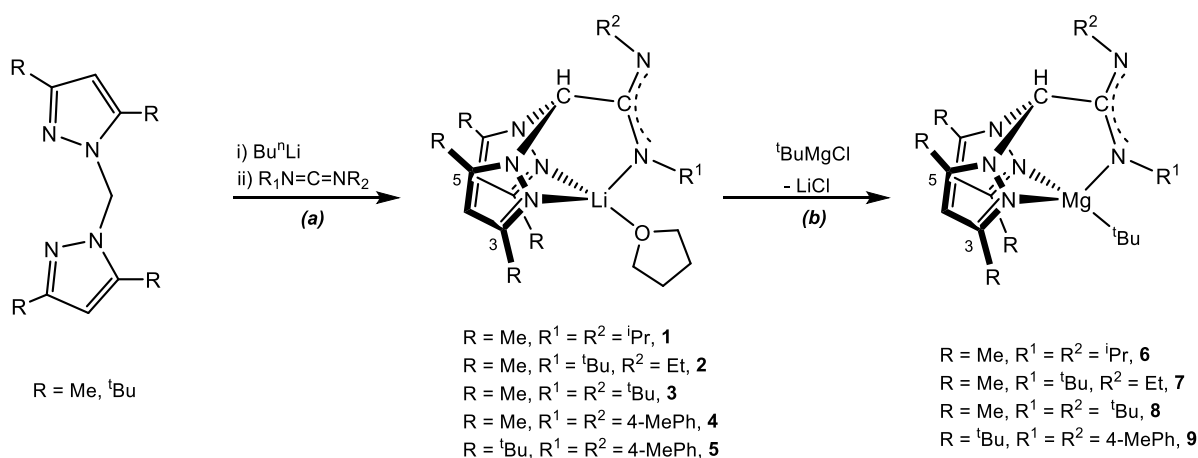
Results and Discussion

Synthesis and Characterization of the Heteroscorpionate Lithium Precursors and the ^tButyl Polynuclear Magnesium Complexes.

In a similar manner to the previously described preparation of the analogous low¹⁵ and high¹⁶ sterically hindered amidinate-based heteroscorpionate lithium starting materials, a mixture of a cooled (–70 °C) solution of bis(3,5-dimethylpyrazol-1-yl)methane (bdmpzm)¹⁵ or bis(3,5-di-*tert*-butylpyrazol-1-yl)methane (bdtbpzm)¹⁶ in THF and one equivalent of BuⁿLi, under an atmosphere of dry nitrogen was treated with the symmetric carbodiimides *N,N'*-di-*tert*-butylcarbodiimide and *N,N'*-1,3-di-*p*-tolylcarbodiimide. These reactions give rise to the new low sterically hindered heteroscorpionate lithium acetamidinates [Li(κ^3 -ttbpamd)(thf)] (**3**) [ttbpamd = *N,N'*-di-*tert*-butylbis(3,5-dimethylpyrazol-1-yl)acetamidinate] and [Li(κ^3 -phbpamd)(thf)] (**4**) [phbpamd = *N,N'*-di-*p*-tolylbis(3,5-dimethylpyrazol-1-yl)acetamidinate], or the high sterically hindered heteroscorpionate lithium acetamidinate [Li(κ^3 -phbp^tamd)(thf)] (**5**) [phbp^tamd = *N,N'*-di-*p*-tolylbis(3,5-di-*tert*-butylpyrazol-1-yl)acetamidinate] as white or pale yellow solids in good yields (*ca.* 85%) after the appropriate work-up (Scheme 1*a*). Complexes **1** and **2** have been described previously.¹⁵

In addition, treatment of the low sterically hindered lithium acetamidinates [Li(κ^3 -pbpamd)(thf)] (**1**), [Li(κ^3 -tbpamd)(thf)] (**2**), [Li(κ^3 -ttbpamd)(thf)] (**3**) and [Li(κ^3 -phbpamd)(thf)] (**4**), and the high sterically hindered lithium acetamidinate [Li(κ^3 -phbp^tamd)(thf)] (**5**), with the Grignard reagent ^tBuMgCl in a 1:1 ratio yielded the magnesium *tert*-butyl derivatives [Mg(^tBu)(κ^3 -NNN)] [NNN = pbpamd (**6**), tbpamd (**7**), ttbpamd (**8**) and, phbp^tamd (**9**)] as pale yellow or white solids in high yields (~80%) (see Scheme 1*b*). Complexes **6** and **7** have been described previously.¹⁵

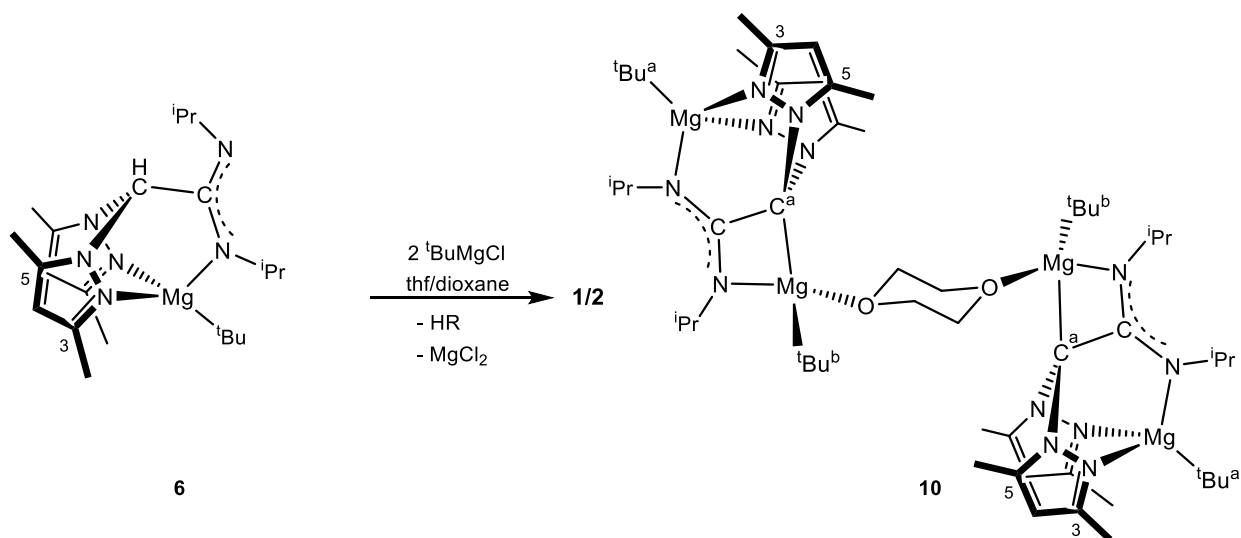
Scheme 1. Sequence of reactions for the preparation of the heteroscorpionate lithium precursors (1–5) and the monoalkyl magnesium complexes (6–9)



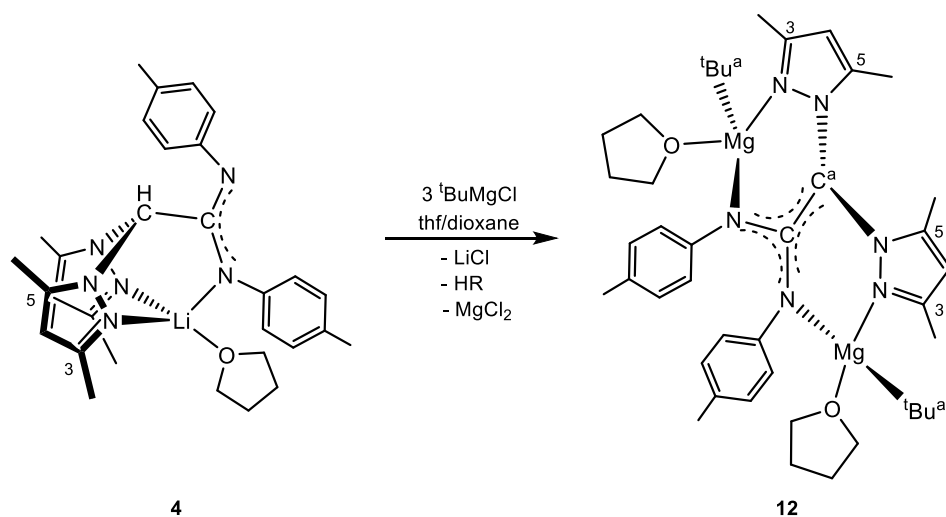
Furthermore, subsequent reaction of the low sterically hindered *tert*-butyl [Mg(^tBu)(κ³-pbpamd)] (**6**) with two additional equivalents of the same ^tBuMgCl in tetrahydrofuran/dioxane (9:1) gave rise to chiral tetranuclear tetraalkyl of the type [{{(^tBu)Mg(κ³-N,N,N;κ²-C,N)Mg(^tBu)}₂{μ-O,O-(C₄H₈)}] (κ³-N,N,N;κ²-C,N = pbpamd⁻ **10**) (See Scheme 2).

Scheme 2. Preparation of the heteroscorpionate tetranuclear tetraalkyl magnesium complex

10



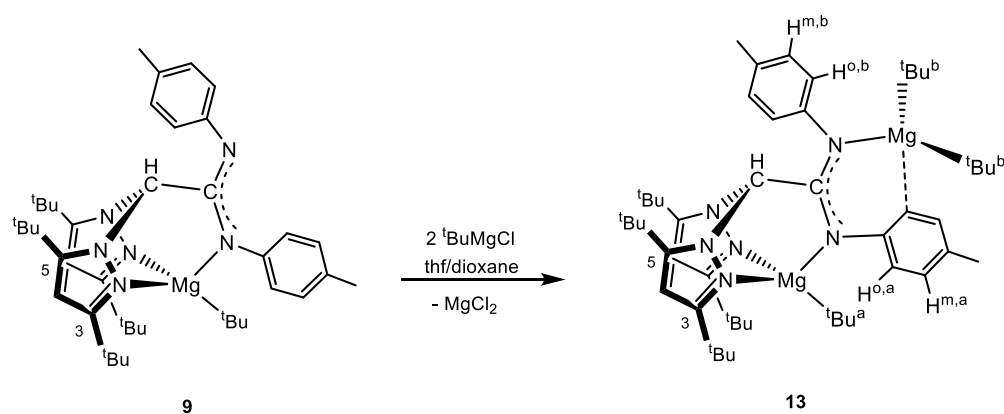
Scheme 4. Preparation of the heteroscorpionate dinuclear dialkyl magnesium complex **12**



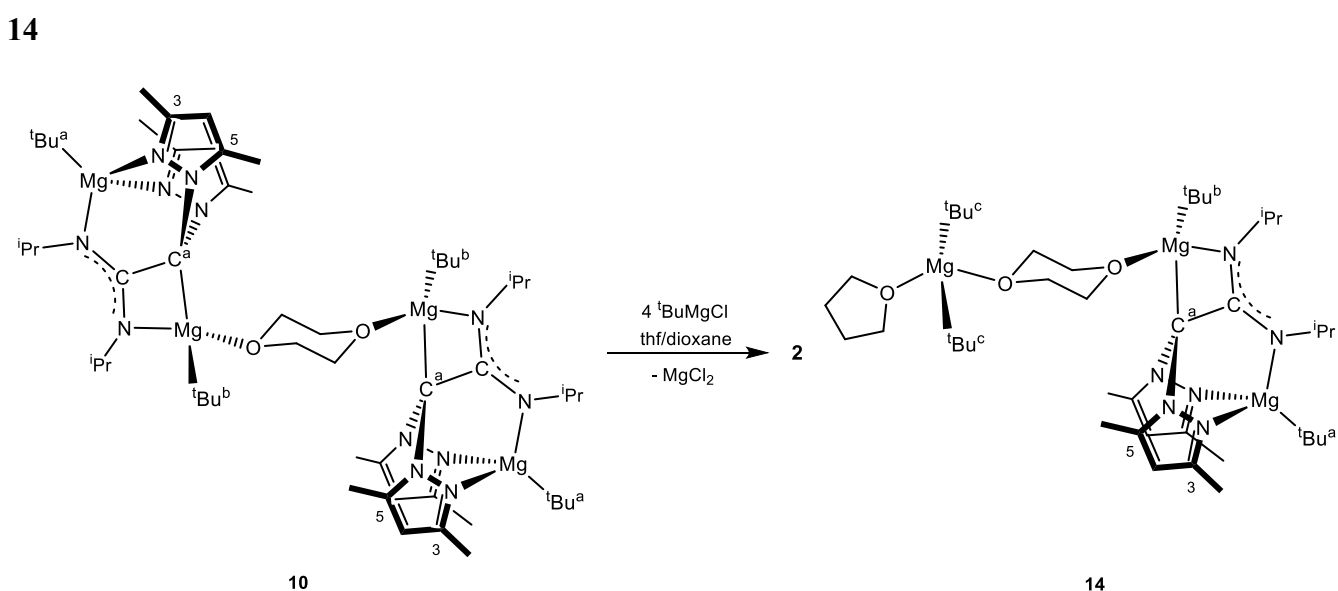
In all cases, *i.e.*, the tetranuclear tetraalkyls **10** and **11a–11b** and the dinuclear dialkyl **12**, an apical C–H methine activation on the scorpionate ligand occurs and this is mediated by the Mg^tBu_2 resulting from the Schlenk equilibrium¹⁴ of the two additional equivalents of Grignard reagent (see Schemes 2–4). It is also interesting to note how the proportion of species arranged as apical $\sigma\text{-C}(sp^3)\text{-Mg}$ versus extended $\pi\text{-C}_2\text{N}_2(sp^2)\text{-Mg}_2$ (**10** and **11a** vs. **11b** and **12**, see Schemes 2–4) varies depending on the substituents on the amidinate fragment in the scorpionate ligands; *e.g.*, pbpamd = 10:0; tbpamd = 8:2 and phbpamd = 0:10. This finding could result from the different Lewis acidities of the bridging methine proton, with *the more acidic the proton producing the more stable extended $\pi\text{-C}_2\text{N}_2(sp^2)\text{-Mg}_2$ covalent bond.*

In contrast to the above, this C–H activation process was not observed for the high sterically hindered *tert*-butyl alkyl **9** but, interestingly, coordination of one additional equivalent of Mg^tBu_2 was observed to afford the dinuclear trialkyl complex $[\text{Mg}(^t\text{Bu})(\kappa^3\text{-phbp}^t\text{amd})\{\text{Mg}(^t\text{Bu})_2\}]$ (**13**) (see Scheme 5), which is the precursor species immediately prior to the apical methine C–H activation. Similarly, the additional coordination of one equivalent of Mg^tBu_2 led to the formation of the chiral trinuclear tetraalkyl species $[\{(^t\text{Bu})\text{Mg}(\text{pbpamd}^-)\text{Mg}(^t\text{Bu})\}\{\mu\text{-}O,O\text{-}(\text{C}_4\text{H}_8)\}\{\text{Mg}(^t\text{Bu})_2(\text{thf})\}]$ (**14**) (see Scheme 6) by cleavage of the dimeric structure of **10**. All compounds were found to be extremely air- and moisture-sensitive and they decomposed when dissolved in dichloromethane.

Scheme 5. Preparation of the heteroscorpionate dinuclear trialkyl magnesium complex 13



Scheme 6. Preparation of the heteroscorpionate trinuclear tetraalkyl magnesium complex 14



The ^1H and $^{13}\text{C}\{-^1\text{H}\}$ NMR spectra of **1–9** in benzene- d_6 at room temperature each show a simple set of resonances for the pyrazole rings, thus indicating the equivalence of these two rings. The amidinate moiety, when $\text{R}_1 = \text{R}_2 = ^t\text{Bu}$ for **3** and 4-MePh for **4** and **5**, gives rise in all cases to two sets of resonances for these substituents, a finding that indicates monodentate binding of the amidinate fragment to the lithium or the magnesium atom (see Scheme 1), in a similar way to the binding modes previously observed for the analogous lithium salt precursors and the corresponding magnesium complexes.^{15,16} In addition, the bridging CH group is also observed as a singlet at low field.

Interestingly, the most significant characteristics in the NMR spectra of **10**, **11a + 11b** and **12** are the disappearance of the original singlet for the CH group in the ^1H NMR spectra and the shift to low field of

this signal in the $^{13}\text{C}\text{-}\{^1\text{H}\}$ NMR spectra (~ 77 ppm), both of which provide evidence for C–H bond activation.

As observed previously in analogous alkyl derivatives,¹⁰ the appearance of a single set of resonances in the ^1H and $^{13}\text{C}\text{-}\{^1\text{H}\}$ NMR spectra for the two pyrazole rings in the chiral tetranuclear tetra-*tert*-butyls **10** and **11a** provide evidence for the equivalence of these rings, despite the lack of symmetry in the molecule due to a possible rapid dynamic exchange between the dioxane and the $^t\text{Bu}^b$ alkyl ligands by rotation around the $\sigma\text{-C}(sp^3)\text{-Mg}$ covalent bond (see Schemes 2 and 3). The VT ^1H NMR studies in toluene-*d*₈ for derivative **10** show a coalescence temperature, T_c , of 203.15 K and a free-energy value, ΔG^\ddagger , of 41.74 kJ/mol [Figure S1 in the Supporting Information (SI)]. These values are consistent with those reported previously for [$\{(\text{CH}_2\text{SiMe}_3)\text{Mg}(\text{tbpamd}^-)\text{Mg}(\text{CH}_2\text{SiMe}_3)\}_2\{\mu\text{-O, O-(C}_4\text{H}_8)\}$] ($T_c = 198.15$, $\Delta G^\ddagger = 40.67$). However, the ^1H NMR spectrum of the chiral tetranuclear tetra-*tert*-butyl **11b** displays two sets of resonances for each of the two pyrazole rings, which indicates that these rings are not equivalent. In addition, the existence of two sets of resonances instead of four provides evidence that only one diastereoisomer (two enantiomers) is present in the isolated bulk solid (see Scheme 3). For the chiral dinuclear di-*tert*-butyl **12**, the signals were reduced to half, thus indicating a symmetrical situation and the presence of only one diastereomer (see Scheme 4). These hypotheses for **11b** and **12** were confirmed by X-ray diffraction analysis.

The amidinate moieties in all of these C–H bond activated complexes [$\text{R}_1 = \text{R}_2 = ^i\text{Pr}$ (**10**), $\text{R}_1 = ^t\text{Bu}$, $\text{R}_2 = \text{Et}$ (**11a + 11b**) and $\text{R}_1 = \text{R}_2 = 4\text{-MePh}$ (**12**)] show two very close sets of resonances in the ^1H NMR spectrum for each R group (*i.e.*, overlapping for the two CH groups in the ^iPr substituents in **10**), in contrast to its corresponding *tert*-butyl precursor [*i.e.*, a difference of ~ 0.9 ppm for the same signals in $[\text{Mg}(^t\text{Bu})(\kappa^3\text{-pbpamd})]$ (**6**)].¹⁵ These observations confirm a bidentate binding of the amidinate fragment to two magnesium centers (see Schemes 2–4). Furthermore, in complexes **10** and **11a + 11b** there are two different signals for each Mg- ^tBu alkyl group ($^t\text{Bu}^a$ and $^t\text{Bu}^b$, see Schemes 2 and 3), which indicates that the two magnesium centers have different arrangements, whereas **12** presents only one set of signals for the two Mg- $^t\text{Bu}^a$ alkyl groups, which confirms the symmetry in the molecule (see Scheme 4). Finally, one

set of signals is observed for the bridging dioxane molecules in **10** and **11a** + **11b**, and for the two terminal tetrahydrofuran ligands in **12**.

Complex **13** shows two sets of signals for the ^tBu groups in the pyrazole rings (^tBu³ and ^tBu⁵) and two different groups of signals for the Mg-^tBu alkyl groups (^tBu^a and ^tBu^b) in a 1:2 ratio, respectively, (see Scheme 5). This observation indicates the existence of a mirror plane in the molecule and this plane includes the amidinate fragment and both magnesium metal centers. More interestingly, the asymmetry in both 4-MePh substituents from the amidinate fragment is evidenced by the shifting of the H^{o,a} and H^{m,a} signals to lower fields by 0.5–0.7 ppm in comparison with H^{o,b} and H^{m,b}. These changes in chemical shift suggest an electron charge transfer from this phenyl group (Ph^a) to the adjacent magnesium center via a $\eta^1-(\pi)$ -C₆H₅ interaction that also occupies the fourth position around the magnesium coordination sphere. Complex **14** presents the same pattern and dynamic behavior as analog **10** and one additional set of signals for the two ^tBu^c groups and for a terminal tetrahydrofuran molecule (see Scheme 6).

In order to confirm the arrangement proposed for each family of complexes, ¹H NOESY-1D experiments were performed to assign unambiguously each signal in all complexes [see Figure S2 in the SI for the assignment of the mixture of **11a** (major) + **11b** (minor)]. The signals for C⁴, Me³ and Me⁵ in the pyrazole rings as well as R, R¹, R² and ^tBu^{a,b,c} in all compounds were assigned by ¹H-¹³C heteronuclear correlations (g-HSQC).

Single crystals of complexes **4**, **6** (the X-ray structure of this complex was determined since it had not previously been established),¹⁵ **8**, **9**, **11b**, **12**, **13** and **14** suitable for X-ray diffraction were easily grown from toluene or hexane solutions at –26 °C. Selected bond lengths and angles are collected in Table 1 for **11b**, **12**, **13** and **14**, and in Table S1 in the SI for **4**, **6**, **8** and **9**. Crystallographic details for all crystal structures are reported in Table S2 in the SI. The molecular structures of **11b**, **12**, **13** and **14** are depicted in Figures 1–4, respectively, and the structures of the complexes **4**, **6**, **8** and **9** are shown in Figures S3–S6 in the SI.

Complexes **11b** and **12** exhibit a centrosymmetric unit cell in which both magnesium centers Mg(1) and Mg(2) are stereogenic, and only the equivalent *meso* diastereomers (*R,S*) were present in the

unit cell. Interestingly, complex **11b** has a dimeric tetranuclear arrangement formed by two twin dinuclear units connected through two bridging dioxane molecules. In contrast, complex **12** is a monomeric dinuclear entity. In the tetranuclear species **11b**, each dinuclear unit contains two different distorted tetrahedral magnesium centers, whereas in the dinuclear complex **12** both analogous magnesium centers are equivalent. In both cases, the magnesium centers are bridged by only one heteroscorpionate ligand; tbpamd⁻ for **11b** and phbpamd⁻ for **12**, which are in a $\kappa^2-N,N;\kappa^2-N,N$ coordination mode and occupy four positions. The N(1)–Mg(1) and N(4)–Mg(2) bond lengths [2.073(6) Å and 2.139(5) Å, respectively, for **11b**] and the N(1,1A)–Mg(1,1A) bond length [2.246(14) Å for **12**] are well-balanced, and the N(6)–Mg(1) and N(5)–Mg(2) bond lengths [2.021(5) Å and 2.039(5) Å, respectively, for **11b**] and the N(5,5A)–Mg(1,1A) bond length [2.013(4) Å for **12**] are slightly shorter than the N(1)–Mg(1) and N(4,1A)–Mg(2,1A) lengths. An additional position around each magnesium atom is occupied in both complexes by a *tert*-butyl group with almost identical Mg–C bond distances [Mg(1)–C(19) = 2.145(7) Å and Mg(2)–C(23) = 2.188(7) Å for **11b**, and Mg(1,1A)–C(20,20A) = 2.119(7) Å for **12**, respectively]. These bond lengths are consistent with those previously observed in analogous heteroscorpionate magnesium alkyls.¹⁰ The fourth position is occupied by the oxygen from a bridging dioxane molecule in **11b** [Mg(1)–O(2A) = 2.121(5) Å and Mg(2)–O(1) = 2.137(5) Å] or a terminal tetrahydrofuran molecule in **12** [Mg(1,1A)–O(1,1A) = 2.039(4) Å, *i.e.* slightly shorter]. However, the most notable feature in the X-ray molecular structures of complexes **11b** and **12** is undoubtedly the delocalization of the carbanion formed as a consequence of the C–H activation. This planar π -extended C₂–N₂ (*sp*²) system is stabilized throughout the adjacent nitrogen atoms. The angles around the central C(12) [N(6)–C(12)–N(5) = 127.6(3)°, N(6)–C(12)–C(11) = 119.0(3)° and N(5)–C(12)–C(11) = 113.4(2)° **11b**; N(5)–C(12)–N(5A) = 123.6(5)°, N(5)–C(12)–C(11) = 118.2(3)° and N(5A)–C(12)–C(11) = 118.2(3)° **12**] are close to 120° and the values are consistent with *sp*² hybridization for C(12). In addition, the N(5)–C(12)–N(6,5A) fragment for **11b** and **12** presents a symmetrical delocalization with nearly equal bond distances [N(5)–C(12) = 1.378(6) Å and N(6)–C(12) = 1.368(7) Å **11b**; 1.365(4) Å **12**]. The C(11)–C(12) bond lengths [1.399(8) Å **11b**; 1.392(8)

Å **12**] are between C–C single (~1.455 Å) and double (~1.339 Å) bonds and this provides evidence for complete π -delocalization throughout the planar C₂–N₂ system. Similar arrangements have been observed previously for Nd¹⁸ and Al¹⁹ complexes supported by enantiopure acetamide and racemic thioacetamide heteroscorpionates, respectively. However, to our knowledge these are the first unambiguously authenticated examples in which these amidinate-heteroscorpionates¹⁵ show this arrangement in the particular case of a magnesium center.

Complex **13** consists of a dinuclear structure formed by two non-symmetrical units. The first magnesium center presents a tetrahedral arrangement that is essentially similar to the one in complex **9** (see Figure S6 in the SI). The heteroscorpionate ligand (phbp^tamd) is in a κ^3 -NNN-coordination mode and occupies three positions [Mg(1)–N(1,3,5) bond distances of 2.200(3), 2.209(3) and 2.110(3) Å, respectively], with the vacant fourth coordination site covered by a ^tBu alkyl group [Mg(1)–C(47) = 2.175(3) Å]. The bond distances and angles are in agreement with those observed in the monomeric complexes cited above. The second Mg(2) unit shows a pseudo tetrahedral arrangement, with initial coordination from the lone pair of electrons on nitrogen N(6) [2.143(3) Å]. The similarity with the N(5)–Mg(1) bond length provides evidence of the complete delocalization of the negative charge throughout the N(5)–C(12)–N(6) core [N(5)–C(12) = 1.324(4) Å, N(6)–C(12) = 1.316(4) Å]. Two additional positions are occupied by two ^tBu alkyl groups, with analogous Mg(2)–C(39,43) bond lengths [2.174(3) Å and 2.161(4) Å, respectively]. Quite unexpectedly, the last coordinative position appears from the interaction of an adjacent phenyl group from the amidinate fragment through a Mg– $\eta^1(\pi)$ -C₆H₅ bond [Mg(2)–C(26) = 2.666(3) Å]. In our opinion, this example represents the immediate precursor species prior to the apical methine C–H activation in the heteroscorpionate ligands – a process that was unsuccessful in this case given the lower Lewis acidity of the bridging methine group in the bis(3,5-di-*tert*-butylpyrazol-1-yl)methane.²³ Interestingly, very few examples of the M– $\eta^1(\pi)$ -C₆H₅ interaction have been reported for early (only for M = Sc, Y,^{24a} La, Ti, Zr, Hf and V) and late (only for M = Fe, Ru, Os,

Co, Rh, Ir, Ni,^{24b} Pd, Pt, Cu, Ag, Au and Hg) transition metals. Thus, as far as we are aware, complex **13** is the first example found for the main group elements and, more specifically, for those of block *s*.

Finally, X-ray diffraction analysis of **14** also confirmed a centrosymmetric unit cell in which the magnesium center Mg(2) is stereogenic. These studies also showed that the presence in solution of the corresponding two enantiomers for this complex (*R* + *S*) was maintained in the solid state. Complex **14** consists of a trinuclear entity formed by two asymmetric units connected through a bridging dioxane molecule. The first asymmetric dinuclear unit, in a similar way to previous heteroscorpionate methanides described by our group,¹⁰ contains two different distorted tetrahedral magnesium centers and the pbpamd⁻ heteroscorpionate ligand. The first metal center contains the heteroscorpionate in a κ^3 -NNN coordination mode occupying three positions, with the N(1)–Mg(1) and N(3)–Mg(1) bond lengths [2.170(2) Å and 2.104(2) Å, respectively] unbalanced and the N(5)–Mg(1) bond length [2.069(2) Å] slightly shorter than N(1,3)–Mg(1). The fourth position is occupied by a *tert*-butyl alkyl group [Mg(1)–C(19) = 2.169(3) Å]. In addition, the N(5)–C(12)–N(6) fragment presents a symmetrical delocalization with nearly equal bond distances [N(5)–C(12) = 1.323(3) Å and N(6)–C(12) = 1.337(3) Å]. These bond lengths are comparable to those observed in the analogous mono¹⁵⁻, di¹⁰⁻ and tetraalkyl¹⁰ magnesium heteroscorpionates. The second magnesium unit, as in the case of **13**, is coordinated by the lone pair of electrons on nitrogen N(6) [N(6)–Mg(2) = 2.029(2) Å] and the similarity with the N(5)–Mg(1) bond length also confirms complete delocalization throughout the N(5)–C(12)–N(6) core. Two additional positions are occupied by the oxygen from a bridging dioxane molecule [Mg(2)–O(1) = 2.145(2) Å] and a ^tBu alkyl group [Mg(2)–C(23) = 2.172(3) Å]. Interestingly, the fourth coordinative vacancy of Mg(2) corresponds to the covalent bond formed between the *sp*³-hybridized apical carbanion C(11) [angles around C(11), such as N(2)–C(11)–N(4) = 107.5(2)°, N(2)–C(11)–C(12) = 107.4(2)° and N(4)–C(11)–C(12) = 115.6(2)°] and the magnesium center Mg(2) [C(11)–Mg(2) = 2.247(3) Å]. In this sense, it is also worth noting that similar unambiguously authenticated examples of C–H activations that result in a methanide carbon with retention of the *sp*³ hybridization and direct Mg–C covalent σ -bond, such as in the

case of amidinate-based di- and tetranuclear heteroscorpionates,¹⁰ are very rare. Indeed, in almost all²⁵ tris-²⁶ and all bis(pyrazol-1-yl)methane^{18,19,27}-based scorpionates the apical carbanion is ‘*naked*’ and these give zwitterionic complexes^{26,27} or, as described above, the carbanion can be delocalized throughout the adjacent heteroatoms.^{18,19} In fact, a few examples of tris(pyrazol-1-yl)methanides with alkaline-earth (Ae) metals have recently been reported and, in these cases, an Ae–C(*sp*³) covalent interaction could not be established, with the exception of calcium.²⁸ Additionally, the similarity in the C(11)–Mg(2) bond length [2.247(3) Å] with the C(19)–Mg(1) and C(23)–Mg(2) [2.169(3) Å and 2.172(3) Å, respectively] bonds mentioned above shows the alkyl character of C(11) and the strong covalent σ -bond between the C(11) and Mg(2) atoms. Moreover, the C(11)–C(12) bond length [1.550(3) Å, *i.e.*, longer than a C–C single bond (~1.455 Å)] reveals the absence of delocalization in the carbanion *sp*³ C(11) between this bond and the close amidinate core, as occurs in the cases of **11b** and **12**. Finally, a highly constrained four-membered metallacycle is formed by the Mg(2)–N(6)–C(12)–C(11) fragment, with highly tensioned angles such as Mg(2)–N(6)–C(12) and Mg(2)–C(11)–C(12) [98.1(1)° and 83.5(1)°, respectively]. These values are far from those expected for *sp*² and *sp*³ hybridization, respectively, but in agreement with those previously observed in analogous alkyl heteroscorpionate methanides.¹⁰ The second asymmetric mononuclear unit consists of a pseudotetrahedral magnesium center with two ^tBu alkyl groups symmetrically coordinated [Mg(3)–C(31) = 2.20(1) Å, Mg(3)–C(35) = 2.167(4) Å] and a terminal tetrahydrofuran molecule [Mg(3)–O(3) = 2.088(2) Å] along with a bridging dioxane molecule [Mg(3)–O(2) = 2.097(2) Å].

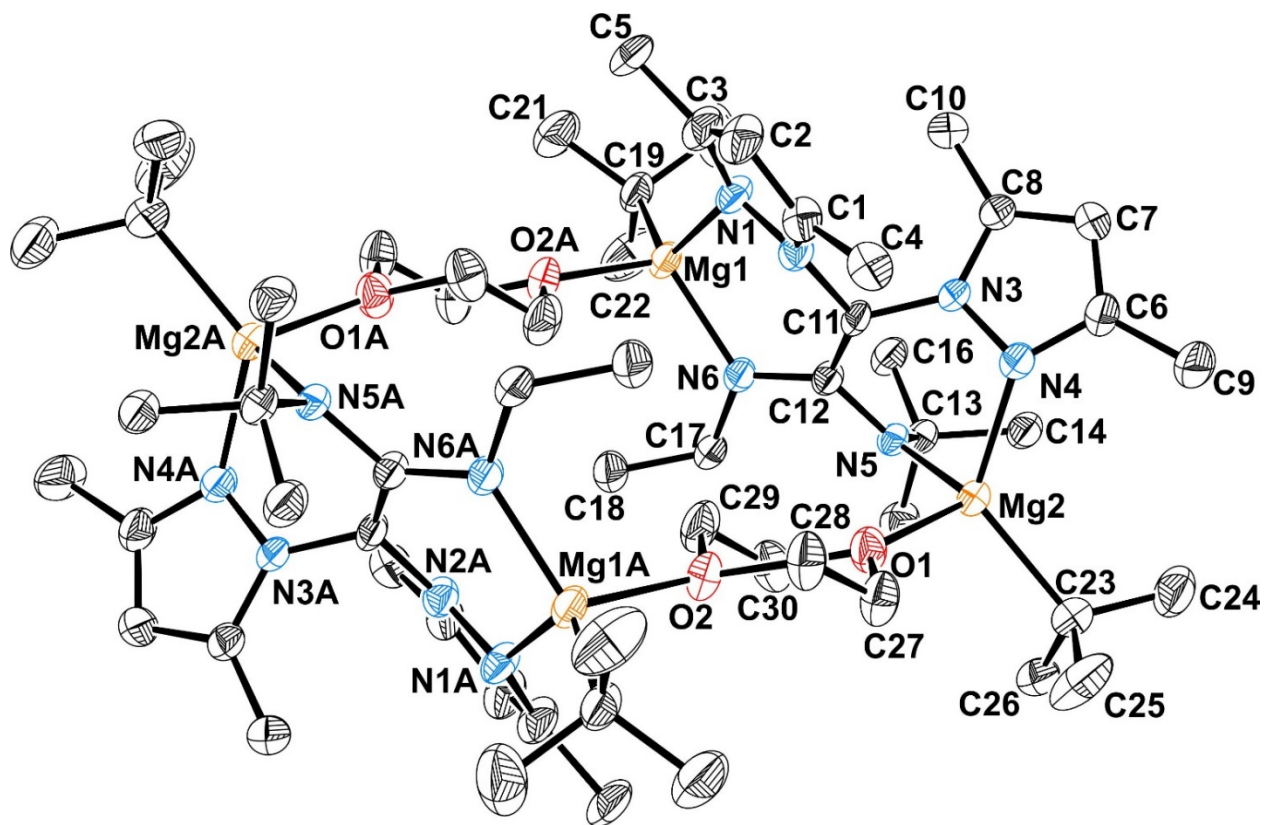


Figure 1. ORTEP view of the *meso* diastereoisomer for $[(^t\text{Bu})\text{Mg}(\text{tbpamd}^-)\text{Mg}(^t\text{Bu})\{\mu\text{-O},\text{O}-(\text{C}_4\text{H}_8)\}]_2$ (**11b**). Hydrogen atoms have been omitted for clarity. Thermal ellipsoids are drawn at the 30% probability level.

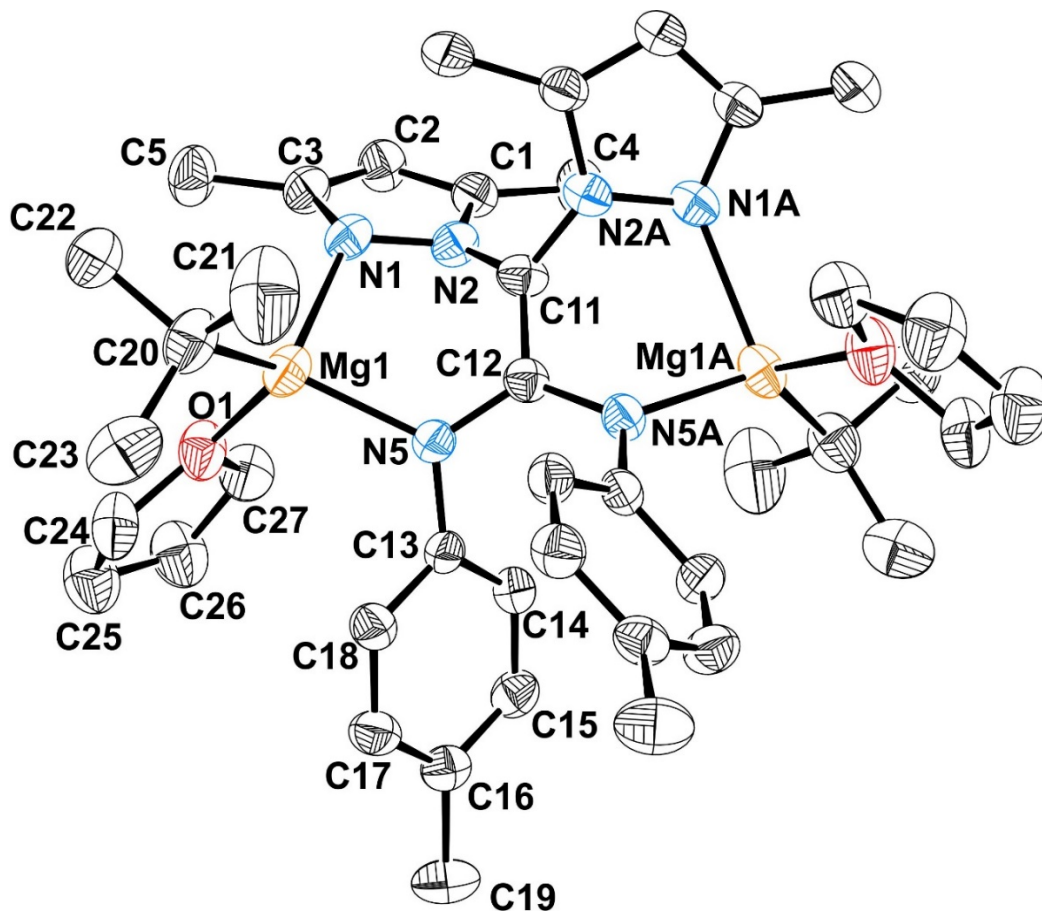


Figure 2. ORTEP view of the *meso* diastereoisomer of [(thf)(^tBu)Mg(phbpamd⁻)Mg(^tBu)(thf)] (12). Hydrogen atoms have been omitted for clarity. Thermal ellipsoids are drawn at the 30% probability level.

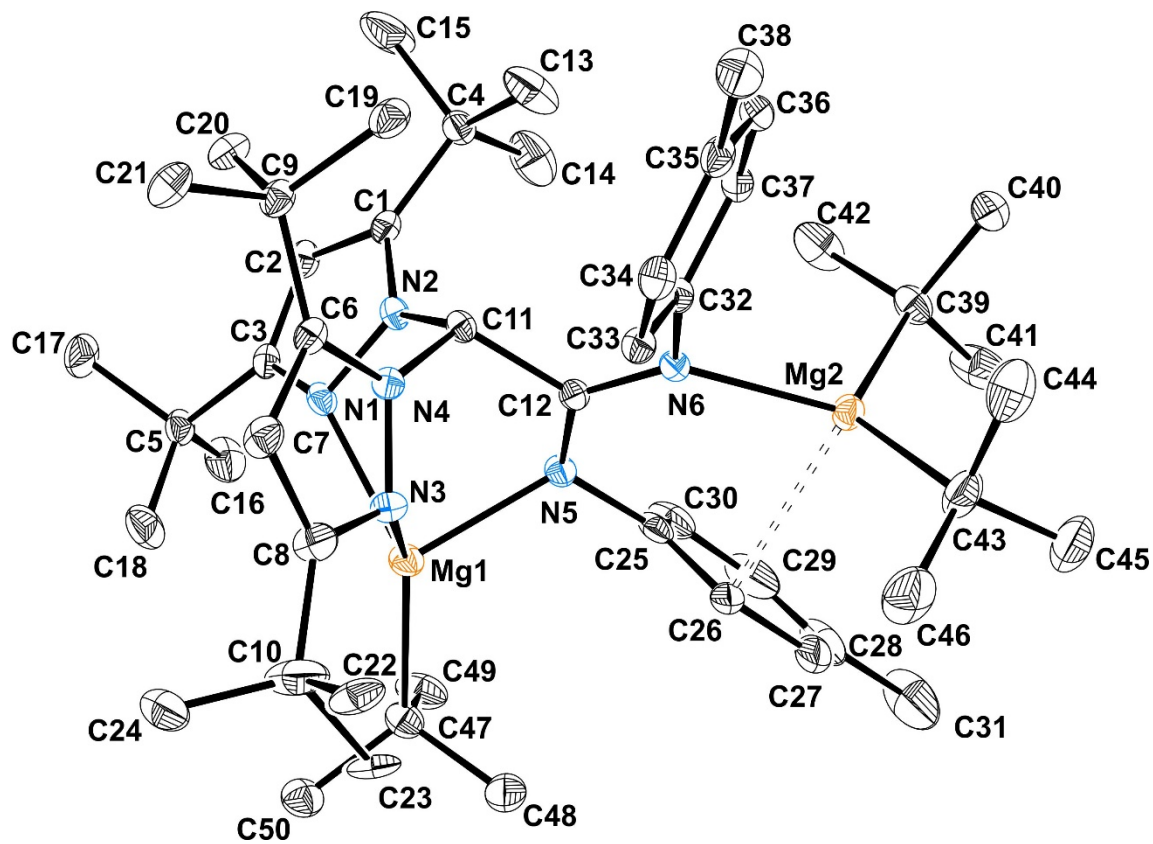


Figure 3. ORTEP view of $[\text{Mg}(\text{tBu})(\kappa^3\text{-phbp'amd})\{\text{Mg}(\text{tBu})_2\}]$ (**13**). Hydrogen atoms have been omitted for clarity. Thermal ellipsoids are drawn at the 30% probability level.

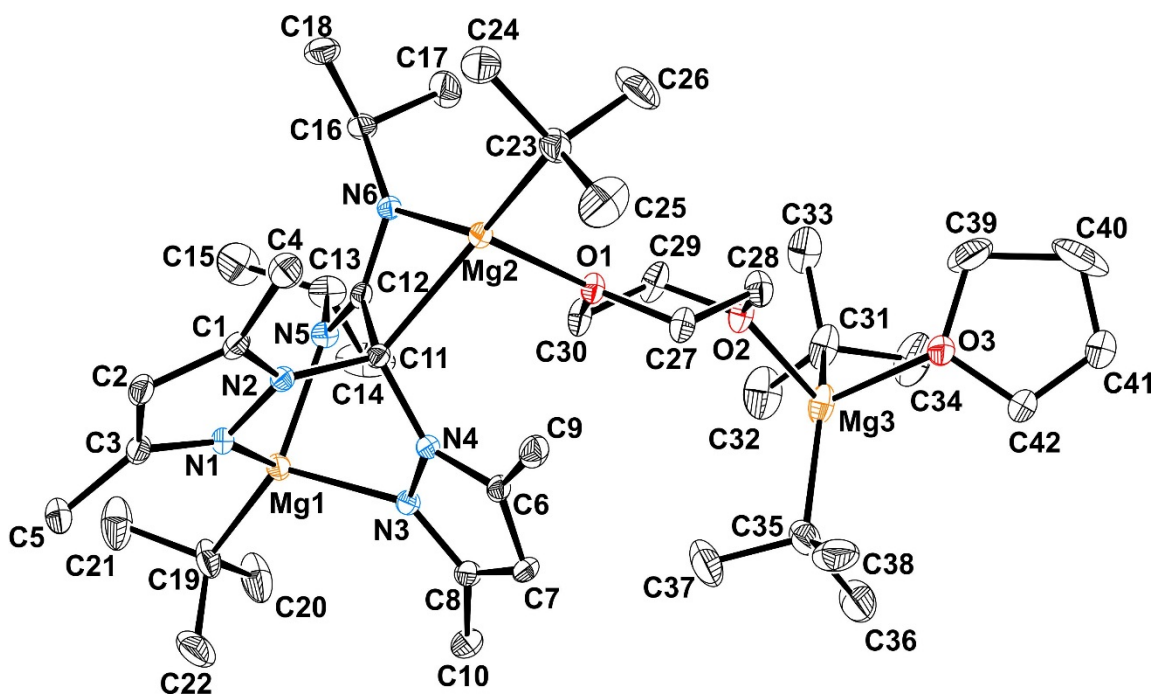


Figure 4. ORTEP view of the *R* enantiomer of $[\{('Bu)Mg(pbpamd^-)Mg('Bu)\}\{\mu-O,O-(C_4H_8)\}\{Mg('Bu)_2(thf)\}]$ (**14**). Hydrogen atoms have been omitted for clarity. Thermal ellipsoids are drawn at the 30% probability level.

Table 1. Bond lengths [\AA] and angles [$^\circ$] for **11b** \times **3(C₇H₈)**, **12**, **13** and **14**.

11b \times 3(C₇H₈)		12		13		14			
<i>Bond Lengths</i>									
Mg(1)-N(1)	2.073(6)	Mg(2)-N(4)	2.139(5)	Mg(1)-N(1)	2.246(14)	Mg(1)-N(1)	2.200(3)	Mg(1)-N(1)	2.170(2)
Mg(1)-N(6)	2.021(5)	Mg(2)-N(5)	2.039(5)	Mg(1)-N(5)	2.013(4)	Mg(1)-N(5)	2.110(3)	Mg(1)-N(3)	2.104(2)
Mg(1)-O(2) ^a	2.121(5)	Mg(2)-O(1)	2.137(5)	Mg(1)-O(1)	2.039(4)	Mg(1)-N(3)	2.209(3)	Mg(1)-N(5)	2.069(2)
Mg(1)-C(19)	2.145(7)	Mg(2)-C(23)	2.188(7)	Mg(1)-C(20)	2.119(7)	Mg(1)-C(47)	2.175(3)	Mg(2)-N(6)	2.029(2)
N(5)-C(12)	1.378(6)			N(5)-C(12)	1.365(4)	Mg(2)-N(6)	2.143(3)	Mg(1)-C(19)	2.169(3)
N(5)-C(13)	1.489(8)			N(5)-C(13)	1.400(5)	Mg(2)-C(26)	2.666(3)	Mg(2)-C(11)	2.247(3)
N(6)-C(12)	1.368(7)			C(11)-C(12)	1.392(8)	N(5)-C(12)	1.324(4)	Mg(2)-O(1)	2.145(2)
N(6)-C(17)	1.474(8)					N(6)-C(12)	1.316(4)	Mg(2)-C(23)	2.172(3)
C(11)-C(12)	1.399(8)					C(11)-C(12)	1.552(4)	N(5)-C(12)	1.323(3)
						Mg(2)-C(39)	2.174(3)	N(6)-C(12)	1.337(3)
						Mg(2)-C(43)	2.161(4)	C(11)-C(12)	1.550(3)
								Mg(3)-C(31)	2.20(1)
								Mg(3)-C(35)	2.167(4)
								Mg(3)-O(2)	2.097(2)
								Mg(3)-O(3)	2.088(2)
<i>Angles</i>									
N(6)-Mg(1)-N(1)	93.0(2)	N(5)-Mg(2)-N(4)	92.0(2)	N(1)-Mg(1)-N(5)	88.2(4)	N(5)-Mg(1)-C(47)	115.5(1)	N(5)-Mg(1)-N(3)	88.11(9)
N(1)-Mg(1)-C(19)	121.8(3)	O(1)-Mg(2)-N(4)	104.9(2)	N(1)-Mg(1)-O(1)	99.0(5)	N(5)-Mg(1)-N(1)	87.2(1)	N(5)-Mg(1)-N(1)	91.30(8)
N(1)-Mg(1)-O(2) ^a	92.0(2)	N(4)-Mg(2)-C(23)	122.3(2)	N(5)-Mg(1)-O(1)	101.7(2)	C(47)-Mg(1)-N(1)	133.4(1)	N(3)-Mg(1)-N(1)	89.48(8)
N(6)-Mg(1)-O(2) ^a	106.7(2)	N(5)-Mg(2)-O(1)	102.4(2)	N(5)-Mg(1)-C(20)	128.0(2)	N(5)-Mg(1)-N(3)	89.3(1)	N(5)-Mg(1)-C(19)	135.8(1)
N(6)-Mg(1)-C(19)	126.0(3)	N(5)-Mg(2)-C(23)	129.4(3)	C(20)-Mg(1)-N(1)	122.0(6)	C(47)-Mg(1)-N(3)	133.0(1)	N(3)-Mg(1)-C(19)	120.7(1)
O(2) ^a -Mg(1)-C(19)	111.3(2)	O(1)-Mg(2)-C(23)	102.7(2)	O(1)-Mg(1)-C(20)	112.3(2)	N(1)-Mg(1)-N(3)	83.80(9)	N(1)-Mg(1)-C(19)	119.2(1)
C(12)-N(5)-C(13)	119.0(5)			C(12)-N(5)-C(13)	118.2(4)	N(5)-Mg(1)-C(12)	25.57(8)	N(6)-Mg(2)-O(1)	97.18(8)

C(12)-N(5)-Mg(2)	114.6(4)	C(12)-N(5)-Mg(1)	120.1(3)	C(47)-Mg(1)-C(12)	138.0(1)	N(6)-Mg(2)-C(23)	135.4(1)
C(13)-N(5)-Mg(2)	123.1(3)	C(13)-N(5)-Mg(1)	121.8(3)	N(1)-Mg(1)-C(12)	77.60(9)	O(1)-Mg(2)-C(23)	104.67(9)
C(12)-N(6)-C(17)	116.4(5)	N(2)a-C(11)-N(2)	110(2)	N(3)-Mg(1)-C(12)	64.97(9)	N(6)-Mg(2)-C(11)	65.81(8)
N(3)-C(11)-N(2)	110.3(5)	N(2)a-C(11)-C(12)	125(1)	N(6)-Mg(2)-C(43)	114.3(1)	O(1)-Mg(2)-C(11)	95.67(8)
C(12)-C(11)-N(2)	125.8(5)	N(2)-C(11)-C(12)	125(1)	N(6)-Mg(2)-C(39)	114.1(1)	C(23)-Mg(2)-C(11)	146.4(1)
C(12)-C(11)-N(3)	121.8(5)	N(5)a-C(12)-N(5)	123.6(5)	N(6)-Mg(2)-C(26)	77.6(1)	N(6)-Mg(2)-C(12)	30.84(8)
N(5)-C(12)-C(11)	114.5(5)	N(5)a-C(12)-C(11)	118.2(3)	C(43)-Mg(2)-C(26)	97.1(1)	O(1)-Mg(2)-C(12)	89.91(7)
N(6)-C(12)-N(5)	125.9(5)	N(5)-C(12)-C(11)	118.2(3)	C(39)-Mg(2)-C(26)	120.7(1)	C(23)-Mg(2)-C(12)	162.8(1)
N(6)-C(12)-C(11)	119.4(5)			C(12)-N(5)-C(25)	118.9(2)	C(11)-Mg(2)-C(12)	36.61(8)
				C(12)-N(5)-Mg(1)	111.0(2)	C(12)-N(5)-C(13)	122.4(2)
				C(25)-N(5)-Mg(1)	119.2(2)	C(12)-N(5)-Mg(1)	115.7(2)
				C(12)-N(6)-C(32)	120.5(2)	C(13)-N(5)-Mg(1)	121.5(2)
				C(12)-N(6)-Mg(2)	130.6(2)	C(12)-N(6)-C(16)	125.8(2)
				C(32)-N(6)-Mg(2)	108.8(2)	C(12)-N(6)-Mg(2)	98.1(1)
				N(4)-C(11)-N(2)	109.9(2)	C(16)-N(6)-Mg(2)	136.0(2)
				N(4)-C(11)-C(12)	112.0(2)	N(2)-C(11)-N(4)	107.5(2)
				N(2)-C(11)-C(12)	110.8(2)	N(2)-C(11)-C(12)	107.4(2)
				N(6)-C(12)-N(5)	126.2(3)	N(4)-C(11)-C(12)	115.6(2)
				N(6)-C(12)-C(11)	120.2(2)	N(2)-C(11)-Mg(2)	128.3(2)
				N(5)-C(12)-C(11)	113.3(2)	N(4)-C(11)-Mg(2)	112.6(1)
						C(12)-C(11)-Mg(2)	83.5(1)
						N(5)-C(12)-N(6)	133.6(2)
						N(5)-C(12)-C(11)	119.0(2)
						N(6)-C(12)-C(11)	107.4(2)
						N(5)-C(12)-Mg(2)	164.0(2)
						N(6)-C(12)-Mg(2)	51.0(1)
						C(11)-C(12)-Mg(2)	59.8(1)

Symmetry transformations used to generate equivalent atoms: ^a -x+2,-y,-z+2;

Polymerization Studies. Complexes **8**, **9**, **10**, **12** and **13** were evaluated in the ring-opening polymerization (ROP) of the polar monomer *rac*-lactide (*rac*-LA) in tetrahydrofuran as solvent under a nitrogen atmosphere. The aim was to compare their activity and stereoselectivity with those of analogous heteroscorpionate methanide magnesium alkyls,^{10,28} other monoalkyls previously reported by our group^{15,16} and some remarkable organo-magnesium initiators published to date, such as the most active magnesium initiator, which consists of a bis(silyl)amido complex supported by a tetradentate monophenolate ligand, communicated by Ma,^{29c} the most heteroselective magnesium initiator containing *n*-butyl and phosphinimino-amino ligands, reported by Cui^{30a}, and other interesting catalysts described in the literature by Chisholm,³¹ Lin³² and Schaper.³³

Initiators **8**, **9**, **10**, **12** and **13** were systematically assessed for the production of poly(*rac*-lactides) (PLAs) (Table 2). The experimental medium-low M_n values of the PLAs produced were in close agreement with the expected theoretical calculated values considering one polymer chain per magnesium center [$M_n(\text{calcd})\text{PLA}_{100} = 14\,400 \text{ g}\cdot\text{mol}^{-1}$] (Table 2). In addition, analysis of the resulting polyesters by size exclusion chromatography (SEC) revealed a monomodal weight distribution, with polydispersities ranging from 1.03 to 1.11 (Figure S7 in the SI).

The alkyl magnesium mononuclear compounds **8** and **9**, tetranuclear compound **10** and the dinuclear compounds **12** and **13** behaved as very active single-component initiators and polymerized 100 equivalents of *rac*-LA in tetrahydrofuran at 20 °C in only a very few hours under otherwise identical conditions.

In particular, mononuclear complex **8** transformed 55% of the monomer after one hour, while the analogous high sterically hindered **9** gave 96% conversion (entries 1 and 6, respectively), probably due to the steric influence of the *tert*-butyl substituents of the heteroscorpionate ligand, which avoids the formation of sandwich species¹⁴ that disfavor catalytic performance.¹⁵ The steric effect of the ^tBu groups in the amidinate fragment can also be appreciated in **8** by comparison with previously reported analogous magnesium monoalkyls,¹⁵ which require more vigorous conditions and much longer reaction times to obtain comparable conversion values (Table 2, entry 9).

In contrast, the tetranuclear complex **10** gave 84% conversion after 5 hours (entry 11) and this proved to be less active than the mononuclear compounds **8** and **9**, probably due to the presence of the dioxane molecule (in **10**), which competes with the magnesium center for the lactide monomer and thus decreases the catalytic activity. Finally, the dinuclear complexes **12** and **13** produced 89 and 74% of polymer after three hours (entries 13 and 15, respectively) and they also gave higher conversions than the tetranuclear compound **10**. Nonetheless, this activity value for **10** was higher than that described previously for analogous tetranuclear magnesium alkyl methanides,¹⁰ since those conversions, even at 50 °C (Table 2, entry 12), are lower than that observed at 20 °C for **10**.

The influence of temperature and solvent was also investigated. As one would expect, when the reaction temperature was 0 °C, the catalytic conversion decreased in all cases (Table 2, entries 7 and 14). Thus, catalyst **9** had a dramatically reduced catalytic activity in toluene (Table 2, entry 8), probably because on using tetrahydrofuran the magnesium ions are complexed by this coordinating solvent, thus leading to an increase in the nucleophilicity of the alkyl initiating group and the alkoxide propagating chains.

The good level of control afforded by these initiators in the polymerization was further exemplified by initiator **9** (entries 2–6), which gave rise to linear correlations between M_n and percentage conversion ($R^2 = 0.991$) (Figure S8 in the SI) in conjunction with narrow molecular weight distributions. This behavior is characteristic of well-controlled living propagations and the existence of a single type of reaction site.

Furthermore, MALDI–ToF MS (Figure S9 in the SI) and end-group analysis by ¹H NMR (Figure S10 in the SI) of low molecular weight poly(*rac*-lactide) oligomers produced by **9** were also investigated. These techniques provided evidence for the initial addition of the *tert*-butyl fragment to the monomer in the materials produced, with subsequent cleavage of the acyl-oxygen bond³⁴ and further monomer additions to the (macro)alcohols.

For the sake of comparison, the most active species **9** (Table 2, entry 6) was much more active than those recently reported by Lin³² for magnesium complexes supported by NNO-tridentate pyrazolonates (78–94% conv, 6–96 hours, 30 °C), by Cui³⁵ for magnesium complexes bearing N,N-

bidentate phenanthrenes (52–96% conv, 20–6 hours, 25–70 °C), by Kozak³⁶ for magnesium amino-bis(phenolato) complexes (16–100% conv, 100–180 min, 125–150 °C), and by Wu³⁷ for binuclear magnesium and zinc alkoxides (93–97% conv, 40–0.33 hours, 25–130 °C). In contrast, the activity was lower than that of the analogous sterically hindered heteroscorpionate magnesium monoalkyls¹⁶ (Table 2, entry 10) [but a significantly higher heteroselectivity was exerted, see below in Poly(*rac*-lactide) Microstructure Analysis)], and still lower than that published by Ma,²⁹ Cui,³⁰ Chisholm,³¹ and Schaper.³³

Table 2. Polymerization of *rac*-Lactide Catalyzed by 8, 9, 10, 12 and 13.^a

entry	initiator	time (h)	yield (g)	conv (%) ^b	$M_{n(\text{theor})}$ (Da) ^c	M_n (Da) ^d	M_w/M_n^d	P_s^e
1	8	1	0.71	55	7 900	7 600	1.07	0.76
2	9	0.2	0.28	22	3 200	3 400	1.05	-
3	9	0.4	0.53	41	5 900	5 300	1.05	-
4	9	0.6	0.76	59	8 500	8 100	1.07	-
5	9	0.8	1.00	77	11 100	11 900	1.08	-
6	9	1	1.24	96	13 800	14 000	1.09	0.85
7	9^f	1	0.68	88	9 800	9 600	1.03	0.85
8	9^g	1	0.57	44	6 300	6 600	1.11	0.82
9	[Mg(CH₂SiMe₃)(pbpamd)]^h	72	0.54	42	6 000	6 800	1.09	atactic
10	[Mg(CH₂SiMe₃)(tbp^hamd)]^h	2.5 (min)	0.65	50	7 200	6 800	1.01	0.79
11	10	5	1.09	84	12 100	12 500	1.10	0.78
12	[{(CH₂SiMe₃)Mg(tbpamd⁻)Mg(CH₂SiMe₃)₂ {μ-O,O-(C₄H₈)}^h}]^h	5	0.98	38	10 900	10 200	1.10	0.78
13	12	3	1.15	89	12 800	12 500	1.09	0.80
14	12^f	3	0.69	53	7 600	7 700	1.04	0.82
15	13	3	0.96	74	10 700	10 600	1.08	0.81

^a Polymerization conditions: 90 μ mol of magnesium centers; [*rac*-LA]₀/[Mg]₀ = 100; 20 mL of tetrahydrofuran at 20 °C. ^b Percentage conversion of the monomer [(weight of polymer recovered/weight of monomer) \times 100]. ^c Theoretical $M_n = (\textit{rac}\text{-LA}/\text{Mg}) \times (\% \text{ conversion}) \times (M_w \text{ of } \textit{rac}\text{-LA})$. ^d Determined by size exclusion chromatography relative to polystyrene standards in tetrahydrofuran. Experimental M_n was calculated considering

Mark–Houwink’s corrections³⁸ for M_n [$M_n(\text{obsd}) = 0.58 \times M_n(\text{GPC})$].^e The parameter P_s (s = syndiotactic) is the probability of forming a new *s*-dyad. P_s is the probability of syndiotactic (racemic) linkages between monomer units and is determined from the relative intensity in the tetrads obtained in the decoupled ¹H NMR experiment by $P_s = 2I_1/(I_1+I_2)$, with $I_1 = \delta$ 5.20–5.25 ppm (*sis, sii/iis*) and $I_2 = \delta$ 5.13–5.20 ppm (*iis/sii, iii, isi*).³⁹

^f The temperature of the polymerization reaction was 0 °C ^g Toluene as solvent. ^h These data have been included for comparison of ROP with the alkyl magnesium precursors. Experimental conditions: *a*) [catalyst]₀ = 90 μmol of [Mg(CH₂SiMe₃)(pbpamd)],¹⁵ [*rac*-LA]₀/[catalyst]₀ = 100, 40 mL of toluene at 70 °C; *b*) [catalyst]₀ = 90 μmol of [Mg(CH₂SiMe₃)(tbp^tamd)],¹⁶ [*rac*-LA]₀/[catalyst]₀ = 100, 10 mL of tetrahydrofuran at 0 °C; *c*) [catalyst]₀ = 90 μmol of magnesium centers in [$\{(\text{CH}_2\text{SiMe}_3)\text{Mg}(\text{tbpamd}^-)\text{Mg}(\text{CH}_2\text{SiMe}_3)\}_2\{\mu\text{-O},\text{O}-(\text{C}_4\text{H}_8)\}$],¹⁰ [*rac*-LA]₀/[Mg]₀ = 200, 20 mL of tetrahydrofuran at 50 °C.

Poly(*rac*-lactide) Microstructure Analysis. Investigation of the microstructure in the poly(*rac*-lactide) by ^1H NMR spectroscopy revealed that these initiators in tetrahydrofuran impart significant heteroactivity on the resulting polymers, possibly through a chain end control⁴⁰ mechanism. The values reached in the tetranuclear and dinuclear species are probably a result of the average contribution of the two different magnesium centers from each initiator (**10**, **12** and **13**).

For instance, the tetranuclear initiator **10** exerts a moderate level of heteroselectivity on the growing polymer microstructure, reaching a P_s ³⁹ value of 0.78 (Table 2, entry 11), whereas the dinuclear compounds **12** and **13** offer a slight but important increase in the heterotactic dyad enchainment ($P_s = 0.82$, Table 2, entry 14) in comparison to that previously found with analogous heteroscorpionate methanides ($P_s = 0.78$, Table 2, entry 12).¹⁰ These findings represent evidence that for the low sterically demanded heteroscorpionate ligands described above, an extended $\pi\text{-C}_2\text{N}_2(\text{sp}^2)\text{-Mg}_2$ arrangement (**12**) exerts a slight increase in heteroactivity in comparison with an apical $\sigma\text{-C}(\text{sp}^3)\text{-Mg}$ disposition (**10**).

More interestingly, the mononuclear catalysts **8** and **9** have a significant hetero-influence on the growing polymer chains. Thus, initiator **8** gave a P_s of 0.76 (Table 2, entry 1) while in the case of **9** the value was 0.85 (Figure S11 in the SI, Table 2, entry 6). This higher heterotacticity observed for **9** is attributed to the more sterically demanding environment produced by the heteroscorpionate phbp'amd. In addition, the behavior observed for **9** is in contrast to that of both heteroscorpionates reported by our group, *i.e.*, the low sterically hindered magnesium monoalkyl precursors, which produced amorphous atactic poly(*rac*-lactide) materials (Table 2, entry 9),¹⁵ and the analogous sterically demanding magnesium monoalkyls¹⁶ ($P_s = 0.79$, Table 2, entry 10). A decrease in the reaction temperature (Table 2, entries 7 and 14) or the use of toluene as solvent (Table 2, entry 8) did not lead to a noticeable increase in the P_s value.

It is also worth mentioning that although the heteroselectivity values observed for catalysts **8**, **9**, **10**, **12** and **13** are lower than that for the highly heteroselective magnesium initiators reported to date, such as the phosphinimino-amino magnesium alkyl prepared by Cui^{30a} ($P_s = 0.98$) or the *nacnac* magnesium alkoxide described by Chisholm^{31a} ($P_s \approx 0.90$), the values found for **9** compare well with those for

benzylalkoxide magnesium complexes supported by NNO-tridentate pyrazolonate ligands reported by Lin³² ($P_s = 0.88$), and they are significantly higher than that for the N,N-bidentate phenanthrene magnesium derivatives reported by Cui³⁵ ($P_s = 0.76$), for magnesium silylamido systems supported by a tridentate monoanionic aminophenolato ligand observed by Ma^{29c} ($P_s = 0.45$), and another sterically hindered diketiminate-based magnesium alkoxide prepared by Schaper³³ ($P_s = 0.45$). More importantly, the values achieved with initiator **9** represent an important step forward in our challenging aim to reach the highest heteroactivity reported to date.

CONCLUSIONS

We report here the particular reactivity found between the low sterically hindered lithium acetamidinates [Li(κ^3 -pbpamd)(thf)], [Li(κ^3 -tbpamd)(thf)], [Li(κ^3 -ttbpamd)(thf)] and [Li(κ^3 -phbpamd)(thf)] and the high sterically demanding [Li(κ^3 -phbp^tamd)(thf)] with the Grignard ^tBuMgCl in different stoichiometries. The initial equimolecular reactions produced the expected magnesium *tert*-butyls of the type [Mg(^tBu)(κ^3 -NNN)]. Interestingly, however, the presence of two additional equivalents of Grignard reagent with several low sterically hindered *tert*-butyl magnesium derivatives in tetrahydrofuran/dioxane gave rise in a controlled manner to different contents of two families of chiral compounds through an apical methine C–H activation process on the heteroscorpionate; the tetranuclear tetraalkyls methanide magnesium complexes [$\{(\text{}^t\text{Bu})\text{Mg}(\kappa^3\text{-}N,N,N;\kappa^2\text{-}C,N)\text{Mg}(\text{}^t\text{Bu})\}_2\{\mu\text{-}O,O\text{-}(C_4H_8)\}$] and the tetranuclear tetraalkyl or the dinuclear dialkyl magnesium complexes [$(\text{}^t\text{Bu})\text{Mg}(\text{tbpamd}^-)\text{Mg}(\text{}^t\text{Bu})\{\mu\text{-}O,O\text{-}(C_4H_8)\}_2$ or $[(\text{thf})(\text{}^t\text{Bu})\text{Mg}(\text{phbpamd}^-)\text{Mg}(\text{}^t\text{Bu})(\text{thf})]$], respectively. The compounds with the more highly Lewis acidic bridging methine proton had the more stable extended $\pi\text{-}C_2N_2(sp^2)\text{-}Mg_2$ covalent bond. Unexpectedly, this C–H activation did not take place in the one example of a high sterically hindered *tert*-butyl isolated, although the coordination of one additional equivalent of Mg^tBu₂ afforded the dinuclear trialkyl complex [Mg(^tBu)(κ^3 -phbp^tamd){Mg(^tBu)₂}], the immediate precursor species prior to the apical methine C–H activation. Similarly, additional coordination of one equivalent of Mg^tBu₂ on a dimeric tetranuclear tetraalkyl

mentioned above produced the chiral trinuclear tetraalkyl species [$\{({}^t\text{Bu})\text{Mg}(\text{pbpamd}^-)\text{Mg}({}^t\text{Bu})\}\{\mu\text{-}O,O\text{-}(\text{C}_4\text{H}_8)\}\{\text{Mg}({}^t\text{Bu})_2(\text{thf})\}$].

Interestingly, the mono-, tetra- and dinuclear alkyl species can act as highly effective single-site living initiators for the well-behaved ROP of *rac*-LA, producing medium-low molecular weight PLA materials in only a few hours even at 0 °C. End group analysis and the MALDI-ToF mass spectra suggest that the polymerization process is initiated by alkyl transfer to the monomer. More importantly, microstructural analysis of the materials showed that an extended $\pi\text{-C}_2\text{N}_2(sp^2)\text{-Mg}_2$ arrangement exerts a slight increase in heteroactivity when compared to an apical $\sigma\text{-C}(sp^3)\text{-Mg}$ disposition in the apical C–H activated multinuclear species. In addition, the highly sterically demanding mononuclear alkyl **9** strongly promotes the formation heterotactic poly(*rac*-lactide), with a P_s value of 0.85.

Experimental Section

General Procedures. All manipulations were carried out under a nitrogen atmosphere using standard Schlenk techniques or a glovebox. Solvents were predried over sodium wire and distilled under nitrogen from sodium (toluene and *n*-hexane) or sodium-benzophenone (THF and diethyl ether). Deuterated solvents were stored over activated 4 Å molecular sieves and degassed by several freeze-thaw cycles. The starting materials bis(3,5-dimethylpyrazol-1-yl)methane (bdmpzm),¹⁵ bis(3,5-di-*tert*-butylpyrazol-1-yl)methane (bdtbpzm),¹⁶ the lithium salts $[\text{Li}(\kappa^3\text{-pbpamd})(\text{thf})]^{15}$ (**1**), $[\text{Li}(\kappa^2\text{-tbpamd})(\text{thf})]^{15}$ (**2**) and the *tert*-butyl magnesium complexes $[\text{Mg}({}^t\text{Bu})(\kappa^3\text{-pbpamd})]^{15}$ (**6**) as well as $[\text{Mg}({}^t\text{Bu})(\kappa^3\text{-pbpamd})]^{15}$ (**7**) were prepared according to the literature procedures. Butyllithium solution, 1,3-di-*p*-tolylcarbodiimide and ${}^t\text{BuMgCl}$ were used as purchased (Aldrich). *rac*-Lactide was sublimed twice, recrystallized from THF and finally sublimed again prior to use.

Instruments and Measurements

NMR spectra were recorded on a Varian Inova FT-500 spectrometer and were referenced to the residual deuterated solvent signal. ^1H NMR homodecoupled and NOESY-1D spectra were recorded on the same instrument with the following acquisition parameters: irradiation time 2 s and 256 scans, using standard VARIAN-FT software. 2D NMR spectra were acquired using the same software and processed using an IPC-Sun computer.

Microanalyses were performed with a Perkin-Elmer 2400 CHN analyzer.

The molecular weights (M_n) and the molecular mass distributions (M_w/M_n) of polymer samples were measured by Gel Permeation Chromatography (GPC) performed on a Shimadzu LC-20AD GPC equipped with a TSK-GEL G3000Hxl column and an ELSD-LTII light-scattering detector. The GPC column was eluted with THF at 40 °C at 1 mL/min and was calibrated using eight monodisperse polystyrene standards in the range 580–483 000 Da.

MALDI-ToF MS data were acquired with a Bruker Autoflex II ToF/ToF spectrometer, using a nitrogen laser source (337 nm, 3 ns) in linear mode with a positive acceleration voltage of 20 kV. Samples were prepared as follows: PLA (20 mg) was dissolved in HPLC quality THF with matrix and NaI in a 100:5:5 ratio. Before evaporation, 10 μL of the mixture solution was deposited on the sample plate. External calibration was performed by using Peptide Calibration Standard II (covered mass range: 700–3 200 Da) and Protein Calibration Standard I (covered mass range: 5 000–17 500 Da). All values are the average of two independent measurements.

The microstructures of PLA samples were determined by examination of the methine region in the homodecoupled ^1H NMR spectrum of the polymers recorded at room temperature in CDCl_3 on a Varian Inova FT-500 spectrometer with concentrations in the range 1.0 to 2.0 mg/mL.

Preparation of Compounds

Synthesis of $[\text{Li}(\kappa^3\text{-ttbpamd})(\text{thf})]$ (3). In a 250 mL Schlenk tube, a solution of Bu^nLi (1.6 M in hexane) (3.06 mL, 4.90 mmol) was added dropwise to a cooled (-70 °C), stirred solution of bdmpzm 30

(1.00 g, 4.90 mmol) in THF (70 mL) and maintained at this temperature over a period of 1 h. *N,N'*-di-*tert*-butylcarbodiimide (0.94 mL, 4.90 mmol) was added dropwise to the previous cooled suspension and the reaction mixture was allowed to warm up to room temperature and the stirring was continued for 1 h. The solvent was evaporated to dryness under reduced pressure and the resulting sticky white product was washed with hexane (40 mL) to give compound **3** as a white solid. Yield: 1.84 g, 86%. Anal. Calcd. For C₂₄H₄₁LiN₆O: C, 66.03; H, 9.47; N, 19.25. Found: C, 66.10; H, 9.45; N, 19.32. ¹H NMR (C₆D₆, 297 K), δ 7.02 (s, 1 H, CH), 5.61 (s, 2 H, H⁴), 3.61 (m, 4 H, THF), 2.06 (s, 6 H, Me⁵), 1.97 (s, 6 H, Me³), 1.86 (s, 9 H, N^tBu), 1.60 (s, 9 H, N^tBu), 1.31 (m, 4H, THF). ¹³C-¹H NMR (C₆D₆, 297 K), δ 150.9 (N=C-N), 147.2, 139.4 (C³ or ⁵), 106.0 (C⁴), 68.6 (THF), 68.3 (CH), 52.1 [C(CH₃)₃], 51.0 [C(CH₃)₃], 34.8 (N^tBu), 30.8 (N^tBu), 25.4 (THF), 13.8 (Me⁵), 11.6 (Me³).

Synthesis of [Li(κ^3 -phbpamd)(thf)] (4). The synthesis of **4** was carried out in an identical manner to **3**. BuⁿLi (1.6 M in hexane) (3.06 mL, 4.90 mmol), bdmpzm (1.00 g, 4.90 mmol), 1,3-di-*p*-tolylcarbodiimide (1.09 g, 4.90 mmol). **4** was obtained as a pale yellow solid. Yield: 2.10 g, 85%. Anal. Calcd. For C₃₀H₃₇LiN₆O: C, 71.41; H, 7.39; N, 16.65. Found: C, 71.52; H, 7.45; N, 16.58. ¹H NMR (C₆D₆, 297 K), δ 7.34 (s, 1 H, CH), 7.02 (m, 8 H, NC₆H₄Me), 5.50 (s, 2 H, H⁴), 3.51 (m, 4 H, THF), 2.21 (s, 6 H, Me⁵), 1.99 (s, 6 H, NC₆H₄Me), 1.81 (s, 6 H, Me³), 1.31 (m, 4 H, THF). ¹³C-¹H NMR (C₆D₆, 297 K), δ 150.0 (N=C-N), 147.9, 140.8 (C³ or ⁵), 140.1-124.0 (NC₆H₄Me), 105.6 (C⁴), 68.2 (THF), 67.5 (CH), 25.5 (THF), 21.0 (NC₆H₄Me), 13.6 (Me⁵), 10.7 (Me³).

Synthesis of [Li(κ^3 -phbp^tamd)(thf)] (5). The synthesis of **5** was carried out in an identical manner to **3**. BuⁿLi (1.6 M in hexane) (1.68 mL, 2.68 mmol), bdtbpzm (1.00 g, 2.68 mmol), 1,3-di-*p*-tolylcarbodiimide (0.60 g, 2.68 mmol). **5** was obtained as a pale yellow solid. Yield: 1.62 g, 90%. Anal. Calcd. For C₄₂H₆₁LiN₆O: C, 74.96; H, 9.14; N, 12.49. Found: C, 74.92; H, 9.18; N, 12.42. ¹H NMR (C₆D₆, 297 K), δ 7.73 (s, 1 H, CH), 6.87 (m, 8 H, NC₆H₄Me), 6.04 (s, 2 H, H⁴), 3.40 (m, 4 H, THF), 2.13 (s, 6 H, NC₆H₄Me), 1.41 (s, 18 H, ^tBu⁵), 1.27 (s, 18 H, ^tBu³), 1.16 (m, 4H, THF). ¹³C-¹H

NMR (C_6D_6 , 297 K), δ 160.3 (N=C–N), 159.3, 153.1 (C^3 or 5), 151.3–122.0 (NC_6H_4Me), 101.9 (C^4), 68.5 (THF), 68.3 (CH), 32.2, 32.1 [$\underline{C}(CH_3)_3$], 30.7 ($^tBu^3$), 30.6 ($^tBu^5$), 25.1 (THF), 21.0 (NC_6H_4Me).

Synthesis of [Mg(tBu)(κ^3 -ttbpamd)] (8). In a 250 cm³ Schlenk tube, compound **3** (1.00 g, 2.29 mmol) was dissolved in dry toluene (70 mL) and cooled to -70 °C. A 1.0 M THF solution of tBuMgCl (2.29 cm³, 2.29 mmol) was added and the mixture was allowed to warm up to room temperature and stirred during 30 min. The suspension was filtered and the resulting yellow solution was concentrated to 20 mL. The solution was cooled to -26 °C and this gave compound **8** as a pale yellow crystalline solid. Yield: 0.83 g, 83%. Anal. Calcd. for $C_{24}H_{42}MgN_6$: C, 65.67; H, 9.64; N, 19.15. Found: C, 65.72; H, 9.68; N, 19.10. 1H NMR (C_6D_6 , 297 K), δ 6.84 (s, 1 H, CH), 5.24 (s, 2 H, H^4), 2.07 (s, 6 H, Me^5), 1.82 [s, 9 H, N–C(\underline{CH}_3)₃], 1.80 (s, 6 H, Me^3), 1.64 [s, 9 H, Mg–C(\underline{CH}_3)₃], 1.43 [s, 9 H, N–C(\underline{CH}_3)₃]. ^{13}C - $\{^1H\}$ NMR (C_6D_6 , 297 K), δ 149.0 (N=C–N), 150.3, 140.5 (C^3 or 5), 107.1 (C^4), 65.1 (CH), 52.4, 51.4 [N– $\underline{C}(CH_3)_3$], 34.8 [Mg–C(\underline{CH}_3)₃], 34.7 [Mg– $\underline{C}(CH_3)_3$], 34.4, 30.9 [N–C(\underline{CH}_3)₃], 13.8 (Me^5), 11.5 (Me^3).

Synthesis of [Mg(tBu)(κ^3 -phbp t amd)] (9). In a 250 cm³ Schlenk tube, compound **5** (1.00 g, 1.49 mmol) was dissolved in dry diethyl ether (70 mL) and cooled to -70 °C. A 1.0 M THF solution of tBuMgCl (1.49 cm³, 1.49 mmol) was added and the mixture was allowed to warm up to room temperature and stirred during 6 h. The suspension was filtered and the resulting yellow solution was concentrated to dryness. The sticky yellow solid was dissolved in hexane (20 mL) and the solution was cooled to -26 °C and this gave compound **9** as a white solid. Yield: 0.79 g, 79%. Anal. Calcd. for $C_{42}H_{62}MgN_6$: C, 74.70; H, 9.25; N, 12.45. Found: C, 74.74; H, 9.20; N, 12.47. 1H NMR (C_6D_6 , 297 K), δ 7.80 (s, 1 H, CH), 6.87 (d, 2 H, $^3J_{H-H}=7.82$ Hz, NC_6H_4Me), 6.74 (d, 2 H, $^3J_{H-H}=7.82$ Hz, NC_6H_4Me), 6.69 (d, 2 H, $^3J_{H-H}=8.22$ Hz, NC_6H_4Me), 6.55 (d, 2 H, $^3J_{H-H}=8.22$ Hz, NC_6H_4Me), 6.01 (s, 2 H, H^4), 2.08 (s, 3 H, NC_6H_4Me), 2.02 (s, 3 H, NC_6H_4Me), 1.36 (s, 18 H, $^tBu^5$), 1.34 (s, 18 H, $^tBu^3$), 1.30 [s, 9 H, Mg–C(\underline{CH}_3)₃]. ^{13}C - $\{^1H\}$ NMR (C_6D_6 , 297 K), δ 164.0 (N=C–N), 155.9, 154.6 (C^3 or 5),

149.5.3-121.8 (NC₆H₄Me), 102.8 (C⁴), 77.1 (CH), 35.2 [Mg–C(CH₃)₃], 31.9 [Mg–C(CH₃)₃], 30.8 (tBu⁵), 30.6 (tBu³), 20.8, 20.9 (NC₆H₄Me).

Synthesis of [tBuMg(pbpamd⁻)Mg^tBu]₂{μ-O,O-(C₄H₈)} (10). In a 250 cm³ Schlenk tube, compound **6** (0.75 g, 1.82 mmol) was dissolved in 100 mL of a mixture of dry THF and 1,4-dioxane in a ratio of 9:1 and it was cooled to –70 °C. A 1.0 M THF solution of tBuMgCl (3.65 cm³, 3.65 mmol) was added to the mixture which was allowed to warm up to room temperature and stirred overnight. The solvent was removed under vacuum and the residue was extracted with hexane (2 × 40 mL). The fractions were combined and the resulting yellow solution was concentrated to 20 mL. The solution was cooled to –26 °C and this gave compound **10** as a yellow solid. Yield: 815 mg (0.76 mmol, 84%). Anal. Calcd. for C₅₆H₁₀₀Mg₄N₁₂O₂: C, 62.82; H, 9.41; N, 15.70. Found: C, 62.86; H, 9.45; N, 15.65. ¹H NMR (C₆D₆, 297 K), δ 5.32 (s, 4 H, H⁴), 3.75 [m, 4 H, ³J_{H-H} = 6.3 Hz, CH–(CH₃)₂], 3.28 (s, 8 H, C₄H₈O₂), 2.16 (s, 12 H, Me⁵), 2.14 (s, 12 H, Me³), 1.73 [s, 18 H, Mg–^aC(CH₃)₃], 1.44 [s, 18 H, Mg–^bC(CH₃)₃], 1.27 [d, 12 H, ³J_{H-H} = 6.3 Hz, CH–(CH₃)₂], 1.03 [d, 12 H, ³J_{H-H} = 6.3 Hz, CH–(CH₃)₂]. ¹³C–{¹H} NMR (C₆D₆, 297 K), δ 169.6 (N=C–N), 147.8, 143.3 (C³ or ⁵), 105.2 (C⁴), 76.5 (C^a), 67.2 (C₄H₈O₂), 47.5 [CH–(CH₃)₂], 46.4 [CH–(CH₃)₂], 35.5 [Mg–^aC(CH₃)₃], 35.4 [Mg–^bC(CH₃)₃], 34.9 [Mg–^aC(CH₃)₃], 34.3 [Mg–^bC(CH₃)₃], 26.5 [CH–(CH₃)₂], 26.3 [CH–(CH₃)₂], 13.8 (Me⁵), 13.0 (Me³).

Synthesis of [tBuMg(tbpamd⁻)Mg^tBu]₂{μ-O,O-(C₄H₈)} (11a) + [(tBu)Mg(tbpamd⁻)Mg(tBu){μ-O,O-(C₄H₈)}]₂ (11b). A mixture of complexes **11a** and **11b** in a molar ratio 8:2 were obtained by following the same procedure described for **10** and employing compound **7** (3.0 g, 7.30 mmol) and tBuMgCl (14.60 cm³, 14.60 mmol). By dissolving the solid mixture of **11a** and **11b** in toluene (15 mL) and cooling the solution to –26 °C, a yellow crystalline solid suitable for X-ray diffraction analysis was obtained, corresponding to **11b** × 3(C₇H₈). Yield for **11b** × 3(C₇H₈): 912 mg (0.63 mmol, 87%). Anal. Calcd. for C₈₁H₁₃₂Mg₄N₁₂O₄: C, 67.79; H, 9.27; N, 11.71. Found: C, 67.81; H, 9.25; N, 11.69. ¹H NMR for **11a** (C₆D₆, 297 K), δ 5.32 (s, 4 H, H⁴), 3.36 [q, 4 H, ³J_{H-H} = 6.3 Hz, CH₂–CH₃], 3.28 (s, 8 H, C₄H₈O₂), 2.18 (s, 12 H, Me⁵), 2.10 (s, 12 H, Me³), 1.71 [s, 18 H, Mg–^cC(CH₃)₃], 1.38 [s, 18 H, 33

Mg-^bC(CH₃)₃], 1.29 [s, 18 H, Mg-^aC(CH₃)₃], 1.07 [t, 12 H, ³J_{H-H} = 6.3 Hz, CH₂-CH₃]. ¹³C-¹H} NMR for **11a** (C₆D₆, 297 K), δ 172.8 (N=C-N), 147.6, 143.3 (C³ or ⁵), 105.0 (C⁴), 76.4 (C^a), 67.2 (C₄H₈O₂), 52.1 [CH₂-CH₃], 46.1 [Mg-^aC(CH₃)₃], 46.0 [Mg-^bC(CH₃)₃], 35.4 [Mg-^aC(CH₃)₃], 35.3 [Mg-^bC(CH₃)₃], 33.0 [Mg-^cC(CH₃)₃], 29.3 [Mg-^cC(CH₃)₃], 19.1 [CH₂-CH₃], 13.6 (Me⁵), 12.9 (Me³). ¹H NMR for **11b** (C₆D₆, 297 K), δ 5.40 (s, 4 H, H⁴), 3.28 (s, 8 H, C₄H₈O₂), 3.21 [q, 4 H, ³J_{H-H} = 6.3 Hz, CH₂-CH₃], 2.18 (s, 6 H, Me³), 2.13 (s, 6 H, Me^{3'}), 2.10 (s, 6 H, Me^{5'}), 2.03 (s, 6 H, Me⁵), 1.68 [s, 18 H, Mg-^cC(CH₃)₃], 1.37 [s, 18 H, Mg-^bC(CH₃)₃], 1.35 [s, 18 H, Mg-^aC(CH₃)₃], 0.95 [t, 12 H, ³J_{H-H} = 6.3 Hz, CH₂-(CH₃)]. ¹³C-¹H} NMR for **11b** (C₆D₆, 297 K), δ 174.6 (N=C-N), 148.3, 147.6, 143.3, 143.1 (C^{3,3'} or ^{5,5'}), 105.5 (C⁴), 76.6 (C^a), 67.2 (C₄H₈O₂), 54.3 [CH₂-CH₃], 44.3 [Mg-^aC(CH₃)₃], 44.1 [Mg-^bC(CH₃)₃], 35.3 [Mg-^aC(CH₃)₃], 35.2 [Mg-^bC(CH₃)₃], 32.8 [Mg-^cC(CH₃)₃], 29.1 [Mg-^cC(CH₃)₃], 18.9 [CH₂-CH₃], 15.1 (Me³), 14.8 (Me^{3'}), 13.6 (Me^{5'}), 12.9 (Me⁵).

Synthesis of [(thf)Mg(^tBu)(phbpamd⁻)Mg(^tBu)(thf)] (12**).** In a 250 cm³ Schlenk tube, compound **4** (1.00 g, 1.97 mmol) was dissolved in 100 mL of a mixture of dry THF and 1,4-dioxane in a ratio of 9:1 and it was cooled to -70 °C. A 1.0 M THF solution of ^tBuMgCl (5.93 cm³, 5.93 mmol) was added to the mixture which was allowed to warm up to room temperature and stirred overnight. The solvent was removed under vacuum and the residue was extracted with toluene (2 × 20 mL). The fractions were combined and the resulting yellow solution was concentrated to 20 mL. The solution was cooled to -26 °C and this gave compound **12** as a pale yellow crystalline solid. Yield: 1.326 g (1.81 mmol, 92%). Anal. Calcd. for C₄₂H₆₂Mg₂N₆O₂: C, 68.95; H, 8.54; N, 11.49. Found: C, 68.99; H, 8.57; N, 11.45. ¹H NMR (C₆D₆, 297 K), δ 6.85 (m, 8 H, NC₆H₄Me), 5.49 (s, 2 H, H⁴), 3.15 [m, 4 H, THF], 2.02 (s, 6 H, Me⁵), 2.01 (s, 6 H, Me³), 1.88 (s, 6 H, NC₆H₄Me), 1.82 [s, 18 H, Mg-^aC(CH₃)₃], 0.81 [m, 4 H, THF]. ¹³C-¹H} NMR (C₆D₆, 297 K), δ 169.8 (N=C-N), 148.8, 144.1 (C³ or ⁵), 142.3-125.8 (NC₆H₄Me), 103.2 (C⁴), 77.5 (C^a), 70.3 (THF), 36.5 [Mg-^aC(CH₃)₃], 32.7 [Mg-^aC(CH₃)₃], 26.4 (THF), 22.3 (NC₆H₄Me), 14.5 (Me⁵), 12.4 (Me³).

Synthesis of [Mg(^tBu)(κ³-phbp^tamd)(Mg^tBu₂)] (13). In a 250 cm³ Schlenk tube, compound **9** (1.0 g, 1.48 mmol) was dissolved in 100 mL of a mixture of dry THF and 1,4-dioxane in a ratio of 9:1 and it was cooled to -70 °C. A 1.0 M THF solution of ^tBuMgCl (2.96 cm³, 2.96 mmol) was added to the mixture which was allowed to warm up to room temperature and stirred overnight. The solvent was removed under vacuum and the residue was extracted with toluene (2 × 20 mL). The fractions were combined and the resulting yellow solution was concentrated to 20 mL. The solution was cooled to -26 °C and this gave compound **13** as a pale yellow crystalline solid. Yield: 1.120 g (1.37 mmol, 93%). Anal. Calcd. for C₅₀H₈₀Mg₂N₆: C, 73.79; H, 9.91; N, 10.33. Found: C, 73.84; H, 9.98; N, 10.29. ¹H NMR (C₆D₆, 297 K), δ 7.28 (dd, 4 H^{o,m}, ³J_{H-H} = 7.65 Hz, ^bNC₆H₄Me), 7.18 (s, 1 H, CH), 6.80 (d, 2 H^o, ³J_{H-H} = 8.21 Hz, ^aNC₆H₄Me), 6.62 (d, 2 H^m, ³J_{H-H} = 8.21 Hz, ^aNC₆H₄Me), 5.93 (s, 2 H, H⁴), 2.15 (s, 3 H, NC₆H₄Me), 1.97 (s, 3 H, NC₆H₄Me), 1.23 (s, 18 H, ^tBu⁵), 1.21 (s, 18 H, ^tBu³), 1.10 [s, 9 H, Mg-^aC(CH₃)₃], 0.84 [s, 18 H, Mg-^b(C(CH₃)₃)₂]. ¹³C-¹H} NMR (C₆D₆, 297 K), δ 166.2 (N=C-N), 157.5, 153.4 (C³ or ⁵), 150.1–118.3 (^{a,b}NC₆H₄Me), 101.3 (C⁴), 77.6 (CH), 35.2 [Mg-^aC(CH₃)₃], 33.1 [Mg-^bC(CH₃)₃], 32.0 [Mg-^aC(CH₃)₃], 31.5 [Mg-^bC(CH₃)₃], 30.4 (^tBu⁵), 30.1 (^tBu³), 21.5, 19.2 (NC₆H₄Me).

Synthesis of [{^tBuMg(pbpmad⁻)Mg^tBu}{μ-O,O-(C₄H₈)}{Mg^tBu₂(thf)}] (14). In a 250 cm³ Schlenk tube, complex **10c** (1.0 g, 0.93 mmol) was dissolved in 100 mL of a mixture of dry THF and 1,4-dioxane in a ratio of 9:1 and it was cooled to -70 °C. A 1.0 M THF solution of ^tBuMgCl (3.73 cm³, 3.73 mmol) was added to the mixture which was allowed to warm up to room temperature and stirred overnight. The solvent was removed under vacuum and the residue was extracted with hexane (2 × 40 mL). The fractions were combined and the resulting yellow solution was concentrated to 20 mL. The solution was cooled to -26 °C and this gave compound **14** as a yellow crystalline solid. Yield: 1.298 g (1.64 mmol, 88%). Anal. Calcd. for C₄₂H₈₀Mg₃N₆O₃: C, 63.85; H, 10.21; N, 10.64. Found: C, 63.89; H, 10.26; N, 10.59. ¹H NMR (C₆D₆, 297 K), δ 5.31 (s, 2 H, H⁴), 3.73 [m, 2 H, ³J_{H-H} = 6.3 Hz, CH-(CH₃)₂], 3.28 (s, 8 H, C₄H₈O₂), 3.15 [m, 4 H, THF], 2.15 (s, 6 H, Me⁵), 2.13 (s, 6 H, Me³), 1.72 [s, 9 H, Mg-^aC(CH₃)₃], 1.42 [s, 9 H, Mg-^bC(CH₃)₃], 1.25 [d, 6 H, ³J_{H-H} = 6.3 Hz, CH-(CH₃)₂], 1.04 [d, 6 H, ³J_{H-H} = 6.3 Hz, CH-(CH₃)₂], 0.83 [m, 4 H, THF], 0.75 [s, 18 H, Mg-^c(C(CH₃)₃)₂]. ¹³C-¹H} NMR 35

(C₆D₆, 297 K), δ 170.7 (N=C–N), 148.9, 142.1 (C³ or ⁵), 104.7 (C⁴), 76.9 (C^a), 70.3 (THF), 67.2 (C₄H₈O₂), 46.3 [CH–(CH₃)₂], 44.2 [CH–(CH₃)₂], 35.5 [Mg-^aC(CH₃)₃], 34.4 [Mg-^bC(CH₃)₃], 34.2 [Mg-^aC(CH₃)₃], 33.9 [Mg-^bC(CH₃)₃], 26.4 (THF), 25.8 [CH–(CH₃)₂], 25.3 [CH–(CH₃)₂], 13.4 (Me⁵), 12.9 (Me³).

Typical Polymerization Procedures.

Polymerizations of *rac*-lactide (LA) were performed on a Schlenk line in a flame-dried round-bottomed flask equipped with a magnetic stirrer. The Schlenk tubes were charged in the glovebox with the required amount of LA and initiator, separately, and then attached to the vacuum line. The initiator and LA were dissolved in the appropriate amount of solvent, and temperature equilibration was ensured in both Schlenk flasks by stirring the solutions for 15 min in a bath. The appropriate amount of initiator was added by syringe and polymerization times were measured from that point. Polymerizations were stopped by injecting a solution of hydrochloric acid in methanol. Polymers were precipitated in methanol, filtered off, redissolved and reprecipitated in methanol, and dried in vacuo to constant weight.

X-ray Crystallographic Structure Determination for Complexes 4, 6, 8, 9, 11b, 12, 13 and 14.

The single crystals of **4** × 0.5(C₄H₈O), **6**, **8**, **9** × 0.5(C₆H₁₄), **11b** × 3(C₇H₈), **12**, **13** and **14** were mounted on a glass fiber and transferred to a Bruker X8 APEX II CCD-based diffractometer equipped with a graphite monochromated MoK α radiation source ($\lambda = 0.71073$ Å). The highly redundant datasets were integrated using SAINT⁴¹ and corrected for Lorentz and polarization effects. Multiscan absorption correction was applied to all intensity data using the program SADABS.⁴² The software package SHELXTL version 6.10⁴³ was used for space group determination. The structures were solved by a combination of direct methods with subsequent difference Fourier syntheses and refined by full matrix least-squares on F² using the SHELX-2013/4 suite.⁴⁴ All non-hydrogen atoms were refined with anisotropic thermal displacements and, using a riding model, all hydrogen atoms were placed, and their positions were constrained relative to their parent atom using the appropriate HFIX command

in SHELXL. Complexes **4**, **11b**, **12**, **13** and **14** showed disorder for some pyrazole, ^tBu groups and some solvent molecules. In each case, the occupancies of the disordered contributors were determined by free variable refinement and then rounded and fixed. The geometric restraints of shelxl were employed to ensure sensible chemical geometries. Complexes **4** and **13** contain additional disordered molecules of solvent (THF and *n*-hexane, respectively) and they could not be satisfactorily modeled. The final refinement was performed with the modification of the structure factors for the electron densities of the remaining disordered solvent regions⁴⁵ (total potential solvent accessible void volume of 720 Å³ for **4** (10.9% of unit cell volume) and 673 Å³ for **13** (12.3% of unit cell volume); 242 electrons for **4** and 152 electrons for **13**). Diffraction data for complexes **11b** and **12** were collected over the full sphere but the obtained crystals were always of poor quality and showed decomposition during the diffraction experiment. Finally, the experiments presented for both complexes were considered as sufficient to resolve the structure from experimental data.

Acknowledgments

We gratefully acknowledge financial support from the Ministerio de Economía y Competitividad (MINECO), Spain (Grant Nos. CTQ2014-52899-R, and CTQ2014-51912-REDC), from the Junta de Comunidades de Castilla-La Mancha, Spain (Grant No. PEII-2014-013-A), and from URJC-Banco Santander, Spain (Grant No. GI_EXCELENCIA, 30VCPIGI14).

Supporting Information Available: Details of VT ¹H NMR experiments, NOESY-1D responses, X-ray diffraction studies of complexes **4**, **6**, **8**, and **9**, ring-opening polymerization of *rac*-lactide and X-ray diffraction experimental details of data collection, refinement, atom coordinates as well as anisotropic displacement parameters for complexes **4**, **6**, **8**, **9**, **11b**, **12**, **13** and **14**. This material is available free of charge via the Internet at <http://pubs.acs.org>.

References

- (1) Ragauskas, A. J.; Williams, C. K.; Davison, B. H.; Britovsek, G.; Cairney, J.; Eckert, C. A.; Frederick, W. J., Jr.; Hallett, J. P.; Leak, D. J.; Liotta, C. L.; Mielenz, J. R.; Murphy, R.; Templer, R.; Tschaplinski, T. The path forward for biofuels and biomaterials. *Science* **2006**, *311*, 484–489.
- (2) Source: European Bioplastics, Institute for Bioplastics and Biocomposites, nova-Institute, 2015. www.bio-based.eu/markets and www.downloads.ifbb-hannover.de
- (3) For reviews in this area see: For reviews in this area see: (a) Galbis, J. A.; García-Martín, M. d. G.; de Paz, V.; Galbis, E. Synthetic Polymers from Sugar-Based Monomers. *Chem. Rev.* **2016**, *116*, 1600–1636; (b) Cameron, D. J. A.; Shaver, M. P. Aliphatic polyester polymer stars: synthesis, properties and applications in biomedicine and nanotechnology. *Chem. Soc. Rev.* **2011**, *40*, 1761–1776; (c) Kiesewetter, M. K.; Shin, E. J.; Hedrick, J. L.; Waymouth, R. M. *Macromolecules* **2010**, *43*, 2093–2107; (d) Stanford, M. J.; Dove, A. P. Stereocontrolled ring-opening polymerisation of lactide. *Chem. Soc. Rev.* **2010**, *39*, 486–494.
- (4) For books in this area see: (a) Jiménez, A.; Peltzer, M.; Ruseckaite, R. *Poly(lactic acid) Science and Technology : Processing, Properties, Additives and Applications*. RSC Polymer Chemistry Series, 2014. (b) Auras, R.; Lim, L.-T. *Poly(lactic acid) : synthesis, structures, properties, processing, and applications*. Wiley: Hoboken, NJ, 2010. (c) Dubois, P.; Coulembier, O.; Raquez, J.-M. *Handbook of ring-opening polymerization*. Wiley-VCH: Weinheim, 2009. (d) Chisholm, M. H.; Zhou, Z. Stereoselective polymerization of Lactide. In *Stereoselective Polymerization with Single Site Catalysts*, Baugh, L. S.; Canich, J. A. M., Eds. CRC Press, Taylor & Francis: Boca Raton, Florida, 2008; pp 645–660.
- (5) Pêgo, A. P.; Siebum, B.; Van Luyn, M. J.; Gallego y Van Seijen, X. J.; Poot, A. A.; Grijpma, D. W.; Feijen J. Preparation of Degradable Porous Structures Based on 1,3-Trimethylene

Carbonate and D,L-Lactide (Co)polymers for Heart Tissue Engineering. *Tissue Eng. Pt. A* **2003**, *9*, 981–994.

- (6) Penco, M.; Donetti, R.; Mendichi, R.; Ferruti, P. New poly(ester-carbonate) multi-block copolymers based on poly(lactic-glycolic acid) and poly(ϵ -caprolactone) segments. *Macromol. Chem. Physic.* **1998**, *199*, 1737–1745.
- (7) (a) Inkinen, S.; Hakkarainen, M.; Albertsson, A.-C.; Södergård, A. From Lactic Acid to Poly(lactic acid) (PLA): Characterization and Analysis of PLA and Its Precursors. *Biomacromolecules* **2011**, *12*, 523–532. (b) Darensbourg, D. J.; Choi, W.; Richers, C. P. Ring-Opening Polymerization of Cyclic Monomers by Biocompatible Metal Complexes. Production of Poly(lactide), Polycarbonates, and Their Copolymers. *Macromolecules* **2007**, *40*, 3521–3523.
- (8) (a) Parkin, G. The bioinorganic chemistry of zinc: synthetic analogues of zinc enzymes that feature tripodal ligands. *Chem. Commun.* **2000**, 1971–1985. (b) Mills, C. F. *Zinc in human biology*, Springer-Verlag, New York, 1989. (c) Cowan, J. A. Ed. *The Biological Chemistry of Magnesium*; VCH: New York, 1995. (d) Campbell, N. A. *Biology*, 3rd ed.; Benjamin/Cummings Publishing Company: Redwood City, CA, 1993; pp 718 and 811.
- (9) (a) Ecochem is a polylactide-based packaging material developed by DuPont–ConAgra. (b) Gruber, P. R.; O'Brien, M. Polyesters III: Applications and Commercial Products. In *Biopolymers*, Volume 4; Doi, Y.; Steinbüchel, A., Eds. Wiley-Blackwell: 2002; pp 235–249. (c) www.natureworkslc.com/Product-And-Applications.aspx.
- (10) Garcés, A.; Sánchez-Barba, L. F.; Fernández-Baeza, J.; Otero, A.; Honrado, M.; Lara-Sánchez, A.; Rodríguez, A. M. Heteroscorpionate Magnesium Alkyls Bearing Unprecedented Apical σ -C(sp³)–Mg Bonds: Heteroselective Ring-Opening Polymerization of *rac*-Lactide. *Inorg. Chem.* **2013**, *52*, 12691–12701.

- (11) (a) Honrado, M.; Otero, A.; Fernández-Baeza, J.; Sánchez-Barba, L. F.; Garcés, A.; Lara-Sánchez, A.; Rodríguez, A. M. Copolymerization of Cyclic Esters Controlled by Chiral NNO-Scorpionate Zinc Initiators. *Organometallics* **2016**, *35*, 189–197. (b) Honrado, M.; Otero, A.; Fernández-Baeza, J.; Sánchez-Barba, L. F.; Garcés, A.; Lara-Sánchez, A.; Rodríguez, A. M. Synthesis and Dynamic Behavior of Chiral NNO-Scorpionate Zinc Initiators for the Ring-Opening Polymerization of Cyclic Esters. *Eur. J. Inorg. Chem.* **2016**, 2562–2572.
- (12) Honrado, M.; Otero, A.; Fernández-Baeza, J.; Sánchez-Barba, L. F.; Garcés, A.; Lara-Sánchez, A.; Rodríguez, A. M. Enantiopure N,N,O-scorpionate zinc amide and chloride complexes as efficient initiators for the heteroselective ROP of cyclic esters. *Dalton Trans.* **2014**, *43*, 17090–17100.
- (13) Otero, A.; Fernández-Baeza, J.; Lara-Sánchez, A.; Sánchez-Barba, L. F. Metal complexes with heteroscorpionate ligands based on the bis(pyrazol-1-yl)methane moiety: Catalytic chemistry. *Coord. Chem. Rev.* **2013**, *257*, 1806–1868.
- (14) Schlenk-type rearrangement reactions (the so called “*Schlenk equilibrium*”: $2 \text{RMgX} \rightleftharpoons \text{MgR}_2 + \text{MgX}_2$) depend on a multitude of factors such as the metal–ligand (R) bond (*e.g.*, for the alkaline-earth metals it generally weakens with increasing metal size: $\text{Mg} > \text{Ca} > \text{Sr} > \text{Ba}$), the steric bulk of the ligand R, the solvent, the temperature, and the concentration of the ‘*Grignard*’(-type) reagent. (a) Michel, O.; Dietrich, H. M.; Litlabø, R.; Törnroos, K. W.; Maichle-Mössmer, C.; Anwander, R. Tris(pyrazolyl)borate Complexes of the Alkaline-Earth Metals: Alkylaluminum Precursors and Schlenk-Type Rearrangements. *Organometallics* **2012**, *31*, 3119–3127. (b) Torvisco, A.; O’Brien, A. Y.; Ruhlandt-Senge, K. Advances in alkaline earth-nitrogen chemistry. *Coord. Chem. Rev.* **2011**, *255*, 1268–1292. (c) Kharasch, M. S. R. O. *Grignard reactions of nonmetallic substances*. Prentice Hall: New York, 1954. (d) Schlenk, W.; Schlenk, W. Über die Konstitution der Grignardschen Magnesiumverbindungen. *Berichte der deutschen chemischen Gesellschaft (A and B Series)* **1929**, *62*, 920–924.

- (15) Sánchez-Barba, L. F.; Garcés, A.; Fajardo, M.; Alonso-Moreno, C.; Fernández-Baeza, J.; Otero, A.; Antiñolo, A.; Tejeda, J.; Lara-Sánchez, A.; López-Solera, M. I. Well-Defined Alkyl Heteroscorpionate Magnesium Complexes as Excellent Initiators for the ROP of Cyclic Esters. *Organometallics* **2007**, *26*, 6403–6411.
- (16) Sánchez-Barba, L. F.; Garcés, A.; Fernández-Baeza, J.; Otero, A.; Alonso-Moreno, C.; Lara-Sánchez, A.; Rodríguez, A. M. Stereoselective Production of Poly(*rac*-lactide) by ROP with Highly Efficient Bulky Heteroscorpionate Alkylmagnesium Initiators. *Organometallics* **2011**, *30*, 2775–2789.
- (17) Zhang, Z.; Cui, D. Heteroscorpionate Rare-Earth Metal Zwitterionic Complexes: Syntheses, Characterization, and Heteroselective Catalysis on the Ring-Opening Polymerization of *rac*-Lactide. *Chem. –Eur. J.* **2011**, *17*, 11520–11526.
- (18) Otero, A.; Fernández-Baeza, J.; Lara-Sánchez, A.; Alonso-Moreno, C.; Márquez-Segovia, I.; Sánchez-Barba, L. F.; Rodríguez, A. M. Ring-Opening Polymerization of Cyclic Esters by an Enantiopure Heteroscorpionate Rare Earth Initiator. *Angew. Chem. Int. Ed.* **2009**, *48*, 2176–2179.
- (19) Otero, A.; Lara-Sánchez, A.; Fernández-Baeza, J.; Alonso-Moreno, C.; Tejeda, J.; Castro-Osma, J. A.; Márquez-Segovia, I.; Sánchez-Barba, L. F.; Rodríguez, A. M.; Gómez, M. V. Straightforward Generation of Helical Chirality Driven by a Versatile Heteroscorpionate Ligand: Self-Assembly of a Metal Helicate by Using CH– π Interactions. *Chem. –Eur. J.* **2010**, *16*, 8615–8619.
- (20) Castro-Osma, J. A.; Lara-Sánchez, A.; North, M.; Otero, A.; Villuendas, P. Synthesis of cyclic carbonates using monometallic, and helical bimetallic, aluminium complexes. *Catal Sci. Technol.* **2012**, *2*, 1021–1026.

- (21) Parris, G. E.; Ashby, E. C. Composition of grignard compounds. VII. Composition of methyl- and tert-butylmagnesium halides and their dialkylmagnesium analogs in diethyl ether and tetrahydrofuran as inferred from nuclear magnetic resonance spectroscopy. *J. Am. Chem. Soc.* **1971**, *93*:5, 1206–1213.
- (22) Seyferth, D. The Grignard Reagents. *Organometallics* **2009**, *28*, 1598–1605.
- (23) Díez-Barra, E.; de la Hoz, A.; Sanchez-Migallon, A.; Tejada, J. Selective lithiation of bis(azol-1-yl)methanes. *J. Chem. Soc., Perkin Trans. I* **1993**, 1079–1083.
- (24) Examples of M– $\eta^1(\pi)$ -C₆H₅ interactions with M = (a) early transition metals, see for example: Rodrigues, A.-S.; Kirillov, E.; Lehmann, C. W.; Roisnel, T.; Vuillemin, B.; Razavi, A.; Carpentier, J.-F. Allyl ansa-Lanthanidocenes: Single-Component, Single-Site Catalysts for Controlled Syndiospecific Styrene and Styrene–Ethylene (Co)Polymerization. *Chem.-Eur. J.* **2007**, *13*, 5548–5565, (b) late transition metals, see for example: Herbert, D. E.; Lara, N. C.; Agapie, T. Arene C–H Amination at Nickel in Terphenyl–Diphosphine Complexes with Labile Metal–Arene Interactions. *Chem.-Eur. J.* **2013**, *19*, 16453–16460.
- (25) There is only one example reported of tris(3,5-dimethylpyrazol-1-yl)methanide with direct C(sp³)-M covalent bond (M = Au). See; Krummenacher, I.; Ruegger, H.; Breher, F. Coinage metal complexes of tris(pyrazolyl)methanide [C(3,5-Me₂pz)₃][−]: κ^3 -coordination vs. backbone functionalisation. *Dalton Trans.* **2006**, 1073–1081.
- (26) (a) Cushion, M. G.; Meyer, J.; Heath, A.; Schwarz, A. D.; Fernández, I.; Breher, F.; Mountford, P. Syntheses and Structural Diversity of Group 2 and Group 12 Tris(pyrazolyl)methane and Zwitterionic Tris(pyrazolyl)methanide Compounds. *Organometallics* **2010**, *29*, 1174–1190. (b) Kuzu, I.; Krummenacher, I.; Hewitt, I. J.; Lan, Y.; Mereacre, V.; Powell, A. K.; Höfer, P.; Harmer, J.; Breher, F. Syntheses, Structures and Electronic Properties of Zwitterionic Iron(II) and Cobalt(II) Complexes Featuring Ambidentate Tris(pyrazolyl)methanide Ligands. *Chem. – Eur. J.* **2009**, *15*, 4350–4365. (c) Kuzu, I.; Nied, D.; Breher, F. Synthesis, Crystal Structures

and Redox Properties of Mixed-Sandwich Complexes of Ruthenium(II) with Cyclopentadienyl and Tris(pyrazolyl)methane Ligands. *Eur. J. Inorg. Chem.* **2009**, 872–879. (d) Bigmore, H. R.; Meyer, J.; Krummenacher, I.; Rügger, H.; Clot, E.; Mountford, P.; Breher, F. Syntheses, Reactivity and DFT Studies of Group 2 and Group 12 Metal Complexes of Tris(pyrazolyl)methanides Featuring “Free” Pyramidal Carbanions. *Chem. –Eur. J.* **2008**, *14*, 5918–5934.

- (27) Zhang, Z.; Cui, D. Heteroscorpionate Rare-Earth Metal Zwitterionic Complexes: Syntheses, Characterization, and Heteroselective Catalysis on the Ring-Opening Polymerization of *rac*-Lactide. *Chem. –Eur. J.* **2011**, *17*, 11520–11526.
- (28) Müller, C.; Koch, A.; Görls, H.; KriECK, S.; Westerhausen, M. Tris(pyrazolyl)methanides of the Alkaline Earth Metals: Influence of the Substitution Pattern on Stability and Degradation. *Inorg. Chem.* **2015**, *54*, 635–645.
- (29) (a) Huang, M.; Pan, C.; Ma, H. Ring-opening polymerization of *rac*-lactide and α -methyltrimethylene carbonate catalyzed by magnesium and zinc complexes derived from binaphthyl-based iminophenolate ligands. *Dalton Trans.* **2015**, *44*, 12420–12431. (b) Song, S.; Ma, H.; Yang, Y. Magnesium complexes supported by salan-like ligands: Synthesis, characterization and their application in the ring-opening polymerization of *rac*-lactide. *Dalton Trans.* **2013**, *42*, 14200–14211. (c) Wang, L.; Ma, H. Highly Active Magnesium Initiators for Ring-Opening Polymerization of *rac*-Lactide. *Macromolecules* **2010**, *43*, 6535–6537.
- (30) (a) Xie, H.; Mou, Z.; Liu, B.; Li, P.; Rong, W.; Li, S.; Cui, D. Phosphinimino-amino Magnesium Complexes: Synthesis and Catalysis of Heteroselective ROP of *rac*-Lactide. *Organometallics* **2014**, *33*, 722–730. (b) Wang, Y.; Zhao, W.; Liu, D.; Li, S.; Liu, X.; Cui, D.; Chen, X. Magnesium and Zinc Complexes Supported by N,O-Bidentate Pyridyl Functionalized Alkoxy Ligands: Synthesis and Immortal ROP of ϵ -CL and L-LA. *Organometallics* **2012**, *31*, 4182–4190.

- (31) (a) Chisholm, M. H.; Gallucci, J.; Phomphrai, K. Coordination Chemistry and Reactivity of Monomeric Alkoxides and Amides of Magnesium and Zinc Supported by the Diiminato Ligand $\text{CH}(\text{CMeNC}_6\text{H}_3\text{-2,6-}^i\text{Pr}_2)_2$. A Comparative Study. *Inorg. Chem.* **2002**, *41*, 2785–2794. (b) Chisholm, M. H.; Huffman, J. C.; Phomphrai, K. Monomeric metal alkoxides and trialkyl siloxides: $(\text{BDI})\text{Mg}(\text{O}^i\text{Bu})(\text{THF})$ and $(\text{BDI})\text{Zn}(\text{OSiPh}_3)(\text{THF})$. Comments on single site catalysts for ring-opening polymerization of lactides. *J. Chem. Soc., Dalton Trans.* **2001**, 222–224.
- (32) Chuang, H-J.; Chen, H-L.; Ye, J-L.; Chen, Z-Y.; Huang, P-L.; Liao, T-T.; Tsai, T-E.; Lin, C-C. Ring-opening polymerization of lactides catalyzed by magnesium complexes coordinated with NNO-tridentate pyrazolonate ligands. *J. Polym. Sci. A Polym. Chem.* **2013**, *51*, 696–707.
- (33) Drouin, F.; Whitehorne, T. J. J.; Schaper, F. $\text{Nacnac}^{\text{Bn}}\text{MgO}^i\text{tBu}$: a diketiminate-based catalyst for the polymerisation of *rac*-lactide with slight isotactic preference. *Dalton Trans.* **2011**, *40*, 1396–1400.
- (34) (a) Sánchez-Barba, L. F.; Hughes, D. L.; Humphrey, S. M.; Bochmann, M. Ligand Transfer Reactions of Mixed-Metal Lanthanide/Magnesium Allyl Complexes with β -Diketimines: Synthesis, Structures, and Ring-Opening Polymerization Catalysis. *Organometallics* **2006**, *25*, 1012–1020. (b) Sánchez-Barba, L. F.; Hughes, D. L.; Humphrey, S. M.; Bochmann, M. Synthesis and Structures of New Mixed-Metal Lanthanide/Magnesium Allyl Complexes. *Organometallics* **2005**, *24*, 5329–5334.
- (35) Gao, B.; Li, D-Z-X.; Cui, Y.; Duan, R.; Pang, X. Magnesium complexes bearing *N,N*-bidentate phenanthrene derivatives for the stereoselective ring-opening polymerization of *rac*-lactides. *RSC Adv.* **2015**, *5*, 440–447.
- (36) Devaine-Pressing, K.; Lehr, J-H.; Pratt, M-E.; Dawe, L-N.; Sarjeant, A-A.; Kozak, C-M. Magnesium amino-bis(phenolato) complexes for the ring-opening polymerization of *rac*-lactide. *Dalton Trans.* **2015**, *44*, 12365–12375.

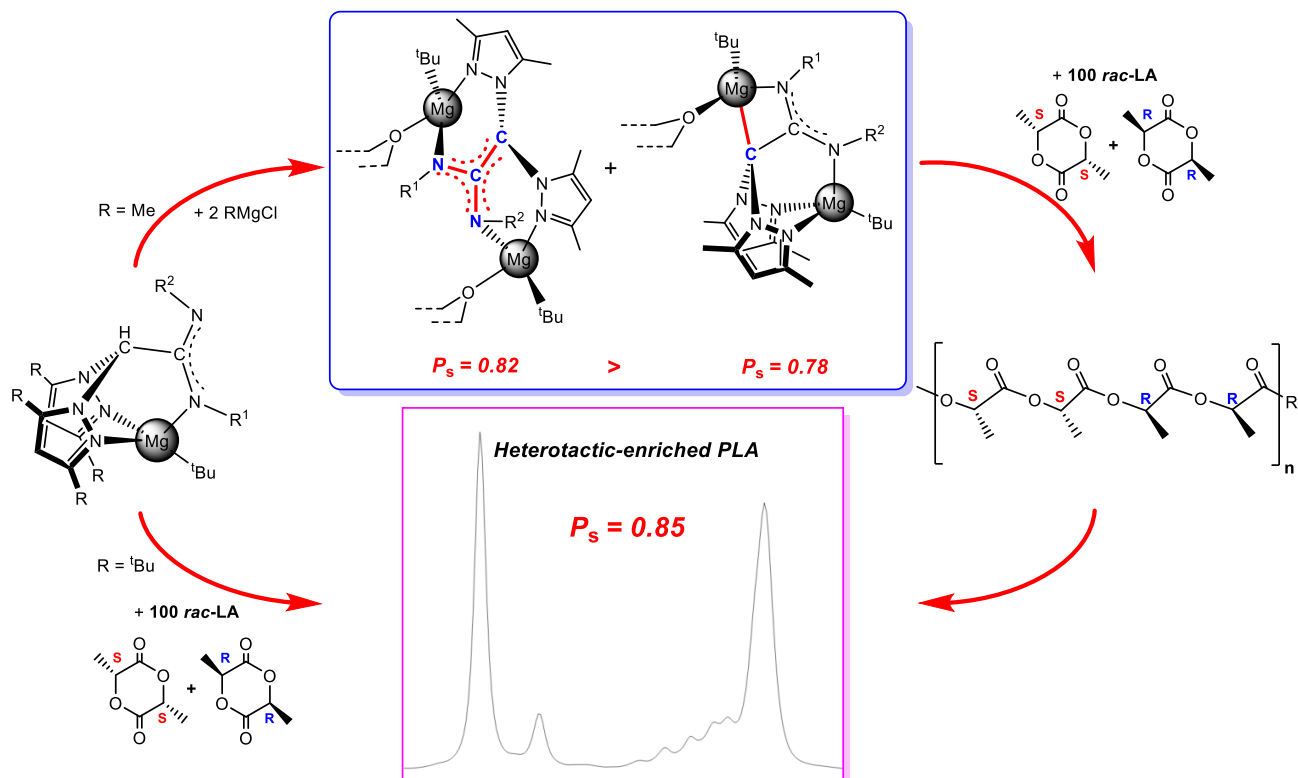
- (37) Sun, Y.; Cui, Y.; Xiong, J.; Dai, Z.; Tang, N.; Wu, J. Different mechanisms at different temperatures for the ring-opening polymerization of lactide catalyzed by binuclear magnesium and zinc alkoxides. *Dalton Trans.* **2015**, *44*, 16383–16391.
- (38) (a) Baran, J.; Duda, A.; Kowalski, A.; Szymanski, R.; Penczek, Intermolecular chain transfer to polymer with chain scission: general treatment and determination of k_p/k_{tr} in L,L-lactide polymerization. *S. Macromol. Rapid Commun.* **1997**, *18*, 325–333. (b) Barakat, I.; Dubois, P.; Jérôme, R.; Teyssié, P. Macromolecular engineering of polylactones and polylactides. X. Selective end-functionalization of poly(D,L)-lactide. *J. Polym. Sci. Pol. Chem.* **1993**, *31*, 505–514.
- (39) (a) Drouin, F.; Oguadinma, P. O.; Whitehorne, T. J. J.; Prud'homme, R. E.; Schaper, F. Lactide Polymerization with Chiral β -Diketiminato Zinc Complexes. *Organometallics* **2010**, *29*, 2139–2147. (b) Chisholm, M. H.; Gallucci, J. C.; Phomphrai, K. Comparative Study of the Coordination Chemistry and Lactide Polymerization of Alkoxide and Amide Complexes of Zinc and Magnesium with a β -Diiminato Ligand Bearing Ether Substituents. *Inorg. Chem.* **2005**, *44*, 8004–8010. (c) Cai, C.-X.; Amgoune, A.; Lehmann, C. W.; Carpentier, J.-F. Stereoselective ring-opening polymerization of racemic lactide using alkoxy-amino-bis(phenolate) group 3 metal complexes. *Chem. Commun.* **2004**, 330–331.
- (40) Nomura, N.; Ishii, R.; Yamamoto, Y.; Kondo, T. Stereoselective Ring-Opening Polymerization of a Racemic Lactide by Using Achiral Salen- and Homosalen-Aluminum Complexes. *Chem. –Eur. J.* **2007**, *13*, 4433–4451.
- (41) SAINT+ v7.12a. Area-Detector Integration Program. Bruker-Nonius AXS. Madison, Wisconsin, USA, 2004.
- (42) Sheldrick, G. M. SADABS version 2004/1. A Program for Empirical Absorption Correction. University of Göttingen, Göttingen, Germany, 2004.

- (43) SHELXTL-NT version 6.12. Structure Determination Package. Bruker-Nonius AXS. Madison, Wisconsin, USA, 2001.
- (44) Sheldrick, G. M. A short history of SHELX. *Acta Crystallogr.*, Sect. A **2008**, *64*, 112–122.
- (45) Spek, A. L. PLATON, An Integrated Tool for the Analysis of the Results of a Single Crystal Structure Determination. *Acta Crystallogr.* **1990**, *A46*, C–34.

**Studies on Multinuclear Magnesium *tert*-Butyl Heteroscorpionates:
Synthesis, Coordination Ability and Heteroselective ROP of *rac*-
Lactide**

Andrés Garcés,[†] Luis F. Sánchez-Barba,^{*†} Juan Fernández-Baeza,[‡] Antonio Otero,^{*‡} Manuel
Honrado,[‡] Agustín Lara-Sánchez,[‡] and Ana M. Rodríguez[‡]

The equimolecular reaction between ^tBuMgCl and new low and high sterically hindered heteroscorpionates [Li(κ^3 -NNN)(thf)] yielded the *tert*-butyls [Mg(^tBu)(κ^3 -NNN)]. Subsequent reaction of the low sterically hindered *tert*-butyls with two additional equivalents of ^tBuMgCl afforded two families of chiral multinuclear compounds in different proportions, in which an apical methine C–H activation process on the heteroscorpionate occurs; the tetranuclear tetraalkyls [$\{({}^t\text{Bu})\text{Mg}(\kappa^3\text{-}N,N,N;\kappa^2\text{-}C,N)\text{Mg}({}^t\text{Bu})\}_2\{\mu\text{-}O,O\text{-}(C_4H_8)\}$], and the tetranuclear tetraalkyl or the dinuclear dialkyl complexes [$({}^t\text{Bu})\text{Mg}(\kappa^2\text{-}N,N;\kappa^2\text{-}N,N)\text{Mg}({}^t\text{Bu})\{\mu\text{-}O,O\text{-}(C_4H_8)\}_2$ or $[(\text{thf})({}^t\text{Bu})\text{Mg}(\kappa^2\text{-}N,N;\kappa^2\text{-}N,N)\text{Mg}({}^t\text{Bu})(\text{thf})]$], respectively, depending on the Lewis acidity of the bridging methine proton. The presence of apical $\sigma\text{-C}(sp^3)\text{-Mg}$ and extended $\pi\text{-C}_2\text{N}_2(sp^2)\text{-Mg}_2$ covalent bonds have been unambiguously confirmed by X-ray analysis. These species can act as highly efficient single-component living initiators for the ROP of *rac*-lactide to produce enhanced levels of heteroselectivity ($P_s = 0.85$).



FOR TABLE OF CONTENTS USE ONLY